SYNTHETIC FEEDBACK LOOP FOR INCREASING MICROBIAL BIOFUEL PRODUCTION USING A BIOSENSOR

A Thesis Presented

by

Mary Harrison

to

The Faculty of the Graduate College

of

The University of Vermont

In Partial Fulfillment of the Requirements
for the Degree of Master of Science
Specializing in Biomedical Engineering

October, 2012

Accepted by the Faculty of the Graduate College, The University of Vermont, in partial fulfillment of the requirements for the degree of Master of Science, specializing in Biomedical Engineering.

Thesis Examination Committee:

_____Advisor
Mary Dunlop, Ph.D.

_____
Jason Bates, Ph.D.

_____Chairperson
Matthew Wargo, Ph.D.

_____Dean, Graduate College
Domenico Grasso, Ph.D.

August 2, 2012

Abstract

Current biofuel production methods use engineered bacteria to break down cellulose and convert it to biofuel. However, this production is limited by the toxicity of the biofuel to the organism that is producing it. Therefore, to increase yields, microbial biofuel tolerance must be increased. Tolerant strains of bacteria use a wide range of mechanisms to counteract the detrimental effects of toxic solvents. Previous research demonstrates that efflux pumps are effective at increasing tolerance to various biofuels. However, when overexpressed, efflux pumps burden cells, which hinders growth and slows biofuel production. Therefore, the toxicity of the biofuel must be balanced with the toxicity of pump overexpression. We have developed a mathematical model and experimentally characterized parts for a synthetic feedback loop to control efflux pump expression so that it is proportional to the concentration of biofuel present. In this way, the biofuel production rate will be maximal when the concentration of biofuel is low because the cell does not expend energy expressing efflux pumps when they are not needed. Additionally, the microbe is able to adapt to toxic conditions by triggering the expression of efflux pumps, which allows it to continue biofuel production. The mathematical model shows that this feedback loop increases biofuel production relative to a model that expresses efflux pumps at a constant level by delaying pump expression until it is needed. This result is more pronounced when there is variability in biofuel production rates because the system can use feedback to adjust to the actual production rate. To complement the mathematical model, we also constructed a whole cell biosensor that responds to biofuel by expressing a fluorescent reporter protein from a promoter under the control of the sensor.

Acknowledgements

I would like to express my gratitude for several individuals who have been instrumental in the completion of my thesis project and my scientific growth. First and foremost, I would like to thank my thesis committee members, including Dr. Bates, Dr. Dunlop, and Dr. Wargo, for their guidance and support throughout this project. In particular, I offer my sincerest thanks to my advisor, Dr. Dunlop, for her patience, flexibility, constant encouragement, and commitment to my scientific development. Special thanks are also due to Dr. Hill and the researchers in the Dunlop and Hill Laboratories for their thoughtful comments and invaluable feedback. In addition to the advancement of my academic pursuits, they have contributed significantly to my enjoyment at the University of Vermont. Finally, I would like to share my great appreciation for my family and friends who provide love and strength in their continual support of my academic endeavors. This project would surely have been impossible without you.

Table of Contents

List of Tables

List of Figures

Chapter 1 Introduction

1.1 Biofuel as a Fuel Source

Transportation accounts for almost 30 percent of energy consumed in the United States, with liquid fuel as the source of the majority of this energy [1]. The rising cost of oil, instability in the oil supply, and the combination of increasing oil use and decreasing petroleum supply have recently raised concerns regarding our dependence on oil for fuel. Additionally, environmental concerns, such as increased carbon emissions, depletion of natural resources, and environmental destruction, emphasize the need for renewable and sustainable energy. These environmental, political, and economic concerns provide a driving force for development of an alternative to fossil fuel based energy sources. Recent developments in synthetic biology and bioengineering suggest that biofuel may be a practical and feasible alternative to current transportation fuels [2].

Previous research has focused on ethanol and it has been successfully implemented as an alternative fuel in Brazil [3]. However, ethanol implementation in high percentages poses several problems in the United States because it is not compatible with current fuel storage and distribution. Therefore, next generation biofuels have gained attention due to their compatibility with existing fuels infrastructure as well as increased energy density and low corrosiveness. Additionally, many next generation biofuels are produced from lignocellosic biomass, which is not used for food products, and therefore does not compete with agricultural resources. Next generation biofuels synthesized by microbes include substitutes for gasoline, diesel, and jet-fuel that have similar properties to current fuel sources [4-8].

1.2   Microbial Biofuel Production

Microbial biofuel production strategies use microorganisms such as *Escherichia coli*, *Saccharomyces cerevisiae*, *Zymomonas mobilis*, and *Clostridium acetobutylicum* to break down cellulosic biomass and convert it into biofuel through fermentation or similar processes [4]. This process is currently optimized by manipulating the genetic makeup of these microorganisms. Native pathways and genes useful for biofuel production are often first identified in environmental isolates. Next, production is either optimized in these isolates or the relevant genes are heterologously expressed in an engineered model organism [9]. Biofuel production is then maximized by focusing the microbe's metabolic processes on the pathways involved in production and eliminating nonessential competing pathways [2].

However, a major barrier to successful and cost competitive production of biofuel, particularly advanced biofuels, is the development of an engineered microbe that is able to produce biofuel at high yields. One of the obstacles facing this objective is that many next-generation biofuels are toxic to microbes. Therefore, the concentration of biofuel achieved is directly limited by the susceptibility of the microbe to the produced biofuel [2, 7, 10-12].

Biofuels may accumulate in the cell membrane, which interferes with multiple vital functions and can ultimately lead to cell death. The presence of biofuel in the membrane increases permeability, which disrupts electrochemical gradients established across the membrane in addition to releasing vital components from the cell. Additionally, biofuels may directly damage biological molecules and trigger an acute

2

stress response [10, 13, 14].

1.3   Tolerance Mechanisms

Some microorganisms possess mechanisms that enable them to tolerate higher concentrations of biofuels. These mechanisms are naturally occurring and are often identified in bacteria living and thriving in hydrocarbon rich environments such as natural oil seepages or oil spills. Tolerance mechanisms include using efflux pumps or membrane vesicles to remove harmful compounds, decreasing membrane permeability, increasing membrane rigidity, and metabolizing the toxic compound [15]. Although many of these mechanisms may be useful in improving microbial tolerance to biofuel, we focus here on efflux pumps and the membrane modifying enzyme *cis*-to-*trans* isomerase because they are known to be present in microbes exhibiting tolerance to hydrocarbons and other compounds structurally similar to biofuels [15].

Efflux pumps are membrane transporters that identify harmful compounds and export them from the cell using the proton motive force [15]. Efflux pumps are capable of identifying a diverse range of compounds and have proven effective at exporting biofuel to improve survival [16, 17]. Although they can be helpful in improving tolerance, if overexpressed, efflux pumps can be detrimental. Overexpression of efflux pumps may alter membrane composition, interrupt ion gradients and transport, and tax membrane integration machinery, which ultimately slows growth [18]. Consequently, when using efflux pumps as a means to increase tolerance to biofuel, the toxicity of pump expression must be managed in addition to biofuel toxicity.

Cis-to-*trans* isomerase (*cti*) is an enzyme that triggers conversion of *cis* fatty acids in the membrane to *trans* fatty acids. Fatty acids in the *trans* orientation are able to pack more tightly together, which increases membrane rigidity and counteracts the fluidity-increasing effects of solvents. This reordering and increased structuring of the membrane occurs as quickly as one minute after exposure. Alternatively, *cti* is constitutively expressed in some organisms and many bacteria living in hydrocarbon rich environments possess higher concentrations of *trans* fatty acids [15, 17, 19-21].

1.4   Feedback Control

Synthetic feedback mechanisms employ elements such as riboswitches [22], transcription factors [23], and genetic toggle switches [24, 25] to control gene expression. Others introduce a synthetic pathway that interacts with native cell functions to introduce and regulate a new response to common molecules [26]. Controllers have also been successfully applied to metabolic networks specifically to increase production of metabolites. This has been accomplished through the use of a toggle switch to monitor changing concentrations of metabolites [25]. Alternatively, biosensors that detect metabolic intermediates have been used to control expression of genes in a production pathway [27, 28].

We propose that using a synthetic feedback loop to control the expression of a tolerance mechanism would balance the toxicity of biofuel production against the adverse effects of overexpression of the tolerance mechanism. We focused on efflux pumps because both their mechanism of tolerance and detrimental effects have been well studied

4

and characterized. Feedback is a common regulatory mechanism used by bacteria to adjust to changing conditions such as fluctuations in nutrient availability, environmental stressors, and signals from other cells in the population. This regulation is often moderated transcriptionally using proteins that bind to a promoter and alter gene expression [29-31].

1.4.1 Sensors

Biosensors are often transcription factors whose activity is modified by changing conditions [32]. Biosensors are capable of responding to a wide range of conditions and compounds, including molecules common to fuels. These biosensors commonly control metabolic pathways or tolerance mechanisms that help the microbe survive in harsh environments. The sensor's activity, activating or repressing a pathway, is in turn controlled by environmental triggers, which alter the sensor's strength. For this study, we have concentrated on MexR, a transcriptional repressor, as a prototypical example of a biosensor.

Many identified sensors have been successfully incorporated into simple genetic circuits for use as whole-cell biosensors, which report the presence or absence of a compound of interest [32, 33]. The feedback mechanism we suggest incorporates a biosensor that responds to biofuel by increasing transcription from an efflux pump operon. The ability of a fuel production host to tune pump expression based on the amount of intracellular biofuel present would balance biofuel and pump expression to optimize survival and yields.

1.4.2   Constant control

An alternative strategy for regulating pump expression would be to use a constant controller (no feedback), such as an inducible promoter. In this way, pump expression could be calibrated to the expected biofuel production rate. Potential advantages of this approach include its simple design and the availability of well-characterized components. However, biological systems exhibit noise and variability [34, 35]. Even genetically identical cells can display significant differences in gene expression. A constant pump system is unable to respond to variations in the system, which would require frequent monitoring and adjustments to tune control to maintain optimal biofuel yield. Therefore a feedback controller, which is able to adapt to changing biofuel production conditions may offer advantages over constant pump expression.

1.5   Thesis Overview

In this work, we explore possible mechanisms to increase tolerance to biofuel for the purpose of increasing biofuel yields from microbial production hosts. First, we consider the utility of a synthetic feedback loop to regulate the expression of tolerance mechanisms, and more specifically efflux pumps. Chapter 2 presents a mathematical model of the biosensor as part of a synthetic feedback loop utilized by a fuel production host. Improvements in biofuel production are observed in comparison to a constant controller. Chapter 3 details the search for a sensor to be incorporated in the model and describes the design and experimental characterization of several biosensors using the transcription factor MexR. Finally, in Chapter 4, we investigate *cis*-to-*trans* isomerase,

6

which alters membrane composition to counteract the detrimental effects of harmful

solvents, as an alternative tolerance mechanism for use in microbial production hosts.

Chapter 2   Synthetic Feedback Control Model Using a Biosensor

2.1   Methods

2.1.1   Feedback controller model development

The model uses the sensor MexR to investigate the utility of a biosensor as a tolerance control mechanism in a synthetic feedback loop. This work motivates the experimental biosensor design described in Chapter 3.. The model was adapted from Dunlop *et al.*, 2010 [36] to include biosensor production and dynamics. It includes a biosensor MexR (*R)* that represses efflux pump expression until it is deactivated in the presence of biofuel (Fig. 1A). The biosensor is regulated by an inducible promoter, P_{lac}, which can be controlled by exogenous addition of isopropyl β-D-1-thiogalactopyranoside (IPTG). MexR works to repress efflux pump expression by binding to the promoter region of the efflux pump operon. When biofuel is present, MexR is deactivated so that it is unable to bind to the promoter and block expression. The model consists of a system of five differential equations representing the relative concentration of important compounds in the bacterium as well as an equation that describes the growth of the overall culture. The dynamics of the system are described by the following system of nonlinear differential equations:

$$\frac{dn}{dt} = \alpha_n n(1 - n) - \delta_n b_i n - \frac{\alpha_n np}{p + \gamma_p}$$

$$\frac{dR}{dt} = \alpha_R + k_R \left(\frac{I}{I + \gamma_I}\right) - \beta_R R$$

$$\frac{dp}{dt} = \alpha_p + k_P \frac{1}{\frac{R}{1 + k_b b_i} + \gamma_R} - \beta_P p$$

8

$$\frac{db_e}{dt} = \delta_b p b_i$$

$$\frac{db_i}{dt} = \alpha_b n - \delta_b p b_i$$

where *n* is the cell density, *R* is the concentration of repressor proteins, *p* is the

concentration of pumps, b_e is the concentration of extracellular biofuel, and b_i is the

concentration of intracellular biofuel.

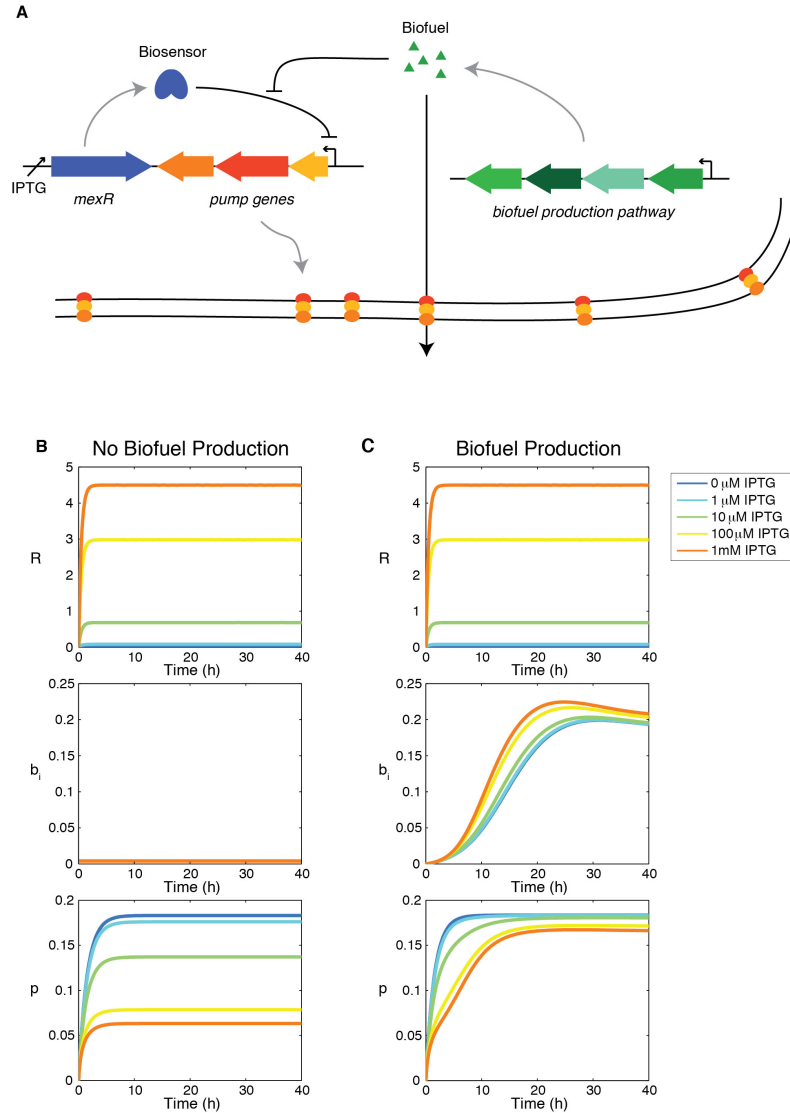Figure 1. Genetic components of the synthetic feedback loop and dynamics of the biosensor. (A) Gene circuit design for the biosensor and synthetic feedback loop. (B) Transient behavior of the feedback model using the biosensor MexR without biofuel production ($\alpha_b = 0$ h^{-1}) and (C) with biofuel production ($\alpha_b = 0.1$ h^{-1}). All other model parameters are as listed in Table 1.

The dynamics for cell growth n model lag, exponential, and stationary phases. Growth is hindered by biofuel toxicity ($\delta_n b_i n$) and pump toxicity ($\frac{\alpha_n n p}{p + \gamma_p}$). Basal production of R and p, given by α_R and α_p, represent the low level of expression that occurs when the promoter is not activated. The degradation rates are given by β_R and β_p. The pump degradation rate β_p includes both active degradation and dilution of the protein as the cells divide. The production rates k_R and k_p represent the strength of expression for R and p, respectively. Repressor activation by an inducer is modeled as $\frac{I}{I + \gamma_I}$, where γ_I indicates the inducer value that corresponds to half maximal activation of repressor. This term models a sigmoidal rise in repressor concentration as the amount of inducer is increased. Repression of efflux pump expression is described as $\frac{1}{\frac{R}{1 + k_b b_i} + \gamma_R}$ where k_b is the equilibrium constant for the deactivation of R and $\frac{R}{1 + k_b b_i}$ represents the amount of active R in the system. Once biofuel is produced intracellularly, we make the simplifying assumption that it may only exit the cell via the action of efflux pumps ($\delta_b p b_i$).

All model parameters are shown in Table 1. The growth rate α_n, biofuel production rate α_b, biofuel toxicity coefficient δ_n, pump protein degradation rate β_P, biofuel export rate δ_b, and pump toxicity threshold γ_p values from (Dunlop, *et al.*, 2010) were used in this model, where δ_n and γ_p were derived from experimental results. The inducer saturation threshold was estimated from the P_{lac} promoter IPTG induction curve [37]. The repressor and pump dynamics are based on MexR's repression of MexAB [38, 39].

Table 1. Parameter values for feedback control model.

Parameter	Description	Value
α_n	Growth rate	$0.66\ \mathrm{h^{-1}}$
α_R	Basal repressor production rate	$0.01\ \mathrm{h^{-1}}$
α_p	Basal pump production rate	$0.01\ \mathrm{h^{-1}}$
α_b	Biofuel production rate	$0.1\ \mathrm{h^{-1}}$
β_R	Repressor degradation rate	$2.1\ \mathrm{h^{-1}}$
β_P	Pump degradation rate	$0.66\ \mathrm{h^{-1}}$
δ_n	Biofuel toxicity coefficient	$0.91\ \mathrm{M^{-1}\ h^{-1}}$
δ_b	Biofuel export rate per pump	$0.5\ \mathrm{M^{-1}\ h^{-1}}$
γ_p	Pump toxicity threshold	0.14
γ_I	Inducer saturation threshold	$60\ \mu\mathrm{M}$
γ_R	Repressor saturation threshold	1.8
k_R	Repressor activation constant	$10\ \mathrm{h^{-1}}$
k_P	Pump activation constant	$0.2\ \mathrm{h^{-1}}$
k_b	Repressor deactivation constant	$100\ \mathrm{M^{-1}}$

2.1.2 Sensitivity analysis

We first asked how dependent modeling results were on system parameters.

Single parameter and two-parameter sensitivity analyses were conducted for the full

feedback controller model by varying the value of each parameter by 20 percent above

and below the nominal values given in Table 1. Sensitivity was calculated as the percent

change in growth caused by altering the variable or combination of variables, as

measured by cell density *n* at 40 hours. For the two-parameter test, all four combinations

of increasing and decreasing each parameter were considered. We define the maximum

change as the greatest change resulting from each combination of parameters. Similarly,

the minimum change is the smallest change resulting from the combination of

parameters. When a parameter was paired with itself, the change caused by altering one

parameter was used.

2.1.3 Constant pump model

In contrast to the feedback model, the constant pump model fixes efflux pump expression at a single level. The constant pump model utilizes an inducer to control pump expression as follows: $\frac{dp}{dt} = \alpha_p + k_p \left(\frac{I}{I+\gamma_I}\right) - \beta_p p$. The repressor equation is removed from the system and the growth n, intracellular biofuel concentration b_i, and extracellular biofuel concentration b_e remain the same as in the biosensor model:

$$\frac{dn}{dt} = \alpha_n n(1-n) - \delta_n b_i n - \frac{\alpha_n n p}{p + \gamma_p}$$

$$\frac{db_e}{dt} = \delta_b p b_i$$

$$\frac{db_i}{dt} = \alpha_b n - \delta_b p b_i .$$

The inducer saturation threshold γ_I, degradation rate β_p, and basal production α_p are the same as used in the biosensor model, but the pump activation constant k_p is set to 0.66 h^{-1}. This value was selected to maximize biofuel production for the parameters given in Table 1. The constant pump model was tuned by setting α_b at 0.1 h^{-1} and varying k_p from 0 to 1.5 hr^{-1} when the model was induced with 10µM IPTG. The value of k_p selected is the one that produced the greatest amount of extracellular biofuel to allow for a controlled comparison against the feedback loop system.

2.1.4 Cell-to-cell variability in biofuel production rate

Cell-to-cell variability was incorporated into system through the biofuel production rate. For 1000 simulations, α_b was chosen randomly from a log-uniform distribution between 0.01 h^{-1} and 1 h^{-1}. The biofuel produced at 40 hours was then

averaged for all simulations. The fully induced sensor model (1mM IPTG) was compared to the constant pump model.

2.2 Results

2.2.1 Sensor dynamics

The feedback system includes a repressor MexR (*R)* that inhibits efflux pump expression until it is deactivated by biofuel. When this occurs, efflux pumps are produced, biofuel is exported, and cells continue to grow and produce biofuel. Transcription of the repressor is activated by an inducer, IPTG, which sets the amount of repressor in the system as well as baseline pump expression (Fig. 1B). It is important to note that the feedback loop design does not require an inducible promoter; this is simply used to tune the system, but could be replaced with a constitutive promoter [40]. When the cells produce biofuel, some of the repressor in the system is deactivated, which inhibits its ability to bind to the efflux pump promoter and repress transcription of the efflux pump operon (Fig. 1C). The total amount of repressor includes activated and unactivated forms and therefore does not change when the cells produce biofuel. Pump expression, however, increases when biofuel is produced as a result of repressor deactivation. The most induced form of the system exhibits the greatest change because it contains the most repressor. The most induced form is also the slowest to reach maximum pump expression. The amount of repressor in the system directly contributes to the sensor's ability to both repress pump expression initially as well as adapt to changing

13

biofuel concentrations. Therefore, the most induced form of the sensor, which exhibits the highest concentration of repressor, is the most responsive.

2.2.2 Sensitivity

Single parameter sensitivity analysis (Fig. 2A) shows that the system is robust to variation in many of the model parameters, however a small subset of influential parameters do impact cell viability. These five parameters—the biofuel toxicity coefficient δ_n, biofuel production rate α_b, biofuel export rate δ_b, growth rate α_n, and pump toxicity threshold γ_p—have the greatest impact on the system when they are varied. The growth rate, pump toxicity threshold, and biofuel toxicity coefficient are based directly on experimental data, but are likely to vary if the bacterial host, efflux pump system, or type of biofuel produced are altered. In contrast to the importance of these five influential parameters, the remaining parameters account for only small changes in cell viability.

Single parameter studies can miss important constructive or destructive effects from the simultaneous variation of parameters. To address this, we conducted a two-parameter sensitivity analysis, which shows that altering parameters in combination can augment (Fig. 2B) or negate (Fig. 2C) the effects of altering a single influential parameter. When two of the influential parameters are altered so that cell growth is decreased or increased, the effect of either parameter individually is reinforced. Similarly if influential parameters are changed so that their effects on growth are opposite, the total change in growth is minimized. This result is not observed for combinations with less influential parameters. The less influential parameters do not alter the change caused by

a major parameter, nor do they produce a considerable change when combined with another minor parameter. This conclusion reinforces the finding from the single parameter analysis that the sensor model is most dependent on a small subset of influential parameters.
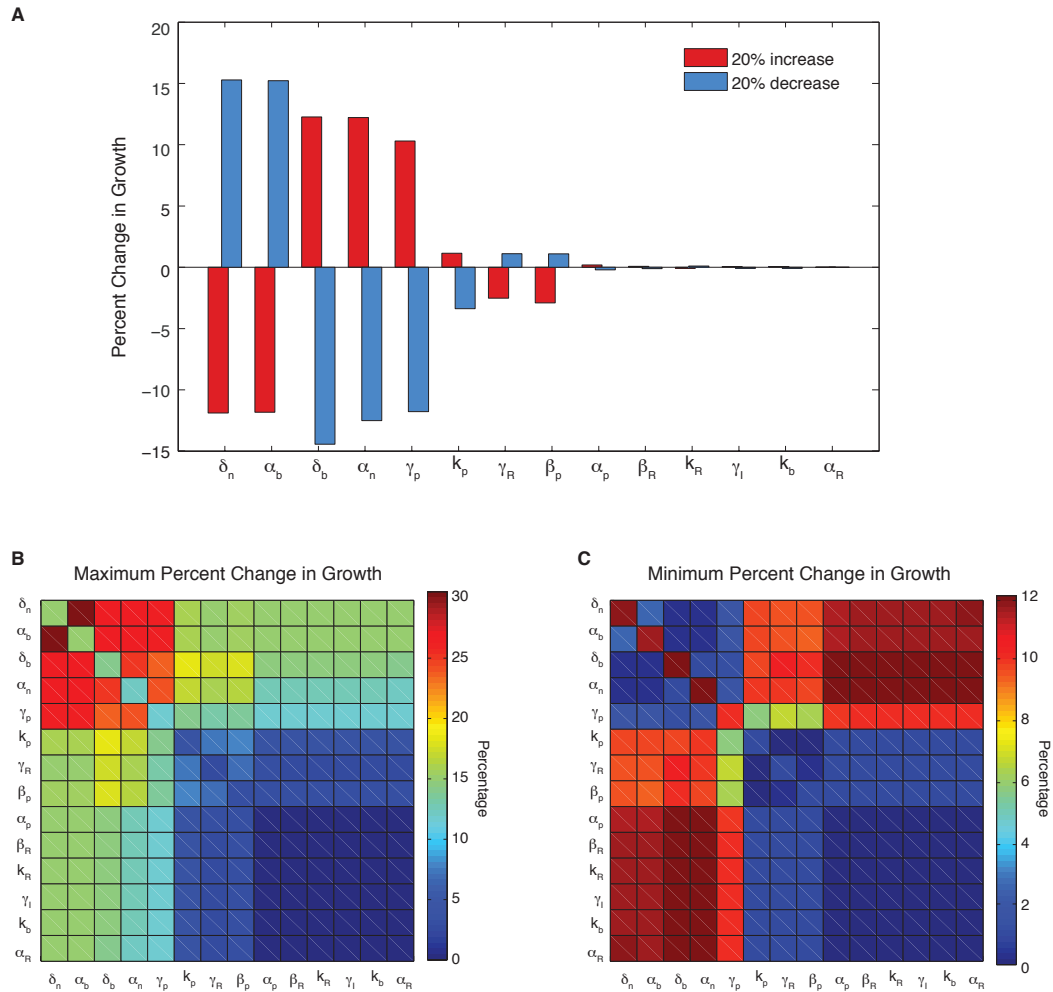

Figure 2. Sensitivity analysis. (A) The percent change in growth for a 20% increase or decrease in a single parameter. (B) The maximum change and (C) minimum change observed for all four combinations of 20% increases and decreases in parameter values for every two-parameter pair. When a parameter is combined with itself, the single parameter change is shown.

2.2.3 Constant pump versus feedback control

Theoretically, in the absence of dynamics and variability, a constant pump system can be tuned so that it performs as well as a controller that incorporates feedback. In fact,

constant controllers have several potential advantages over feedback controllers. They are simpler to build and it is easier to predict behavior because they require fewer components. Additionally, they may be tuned using inducible promoters, which are well characterized and readily available. In practice, however, systems exhibit dynamic behavior as well as cell-to-cell variability, which make perfect tuning of a constant controller impossible [34, 35]. Therefore a feedback controller that is able to tune itself would be advantageous in realistic production systems.

Figure 3 compares the feedback model dynamics to the constant pump model. For all biofuel production rates, the most highly induced sensor model produces the most biofuel. The feedback model's high biofuel production is due to the system's ability to delay efflux pump expression until intracellular biofuel has reached a toxic level. This delay allows the system to grow efficiently, reach a higher population density, and have more cells producing biofuel at a maximal rate because energy is not wasted expressing efflux pumps before they are needed.

As the biofuel production rate is increased (Fig. 3A-C), the delay in pump expression displayed by the most induced form of the sensor decreases because intracellular biofuel accumulates more quickly and efflux pumps are needed earlier. Additionally, pump expression for the sensor increases to accommodate the higher biofuel production rate while pump expression in the constant pump model remains steady. As the biofuel production rate α_b is increased, the feedback model produces the most biofuel by balancing the toxicity of biofuel with the detrimental effects of pump expression. Increasing pump expression aids overall production by decreasing toxicity, which enables cells to grow, balancing production and export. The constant pump model

16

is unable to adapt to export levels. Therefore, even when both models produce a similar amount of intracellular biofuel (Fig. 3C), the sensor model is able to export more biofuel (Fig. 3D).

For a single cell, the sensor model's performance is similar to the constant pump model (Fig. 3A-C). However, the full effect of faster early growth and the ability to adjust to changes in the biofuel production rate are best displayed by looking at the relative biofuel production for the population. Although cells produce similar levels of biofuel, the population size for the feedback system is larger earlier and therefore more total biofuel is produced. Figure 3D shows how the feedback model compares to the constant pump model as a function of the biofuel production rate α_b. The increased overall production due to faster growth rate caused by delayed pump expression is observed by comparing the most induced form of the sensor model to the constant pump model at 0.1 h^{-1}, which, by design, is the optimal production rate for the constant pump model. The constant pump model is not able to do as well as the feedback model once the biofuel production rate for which it is tuned is surpassed.

Next we tested how cell-to-cell variability in biofuel production rates influences biofuel yields. Studies have shown that substantial variability in gene expression exists at the single-cell level [34, 35], suggesting that biofuel production is unlikely to be uniform across a population of cells. Figure 3E shows that the sensor is better suited than the constant pump when the biofuel production rate varies. The large standard deviation in both models results from the variation in biofuel production rates. Importantly, the average biofuel produced for the feedback model is higher, on average, when α_b is

17

variable, which shows that the feedback model's ability to adapt to changing biofuel

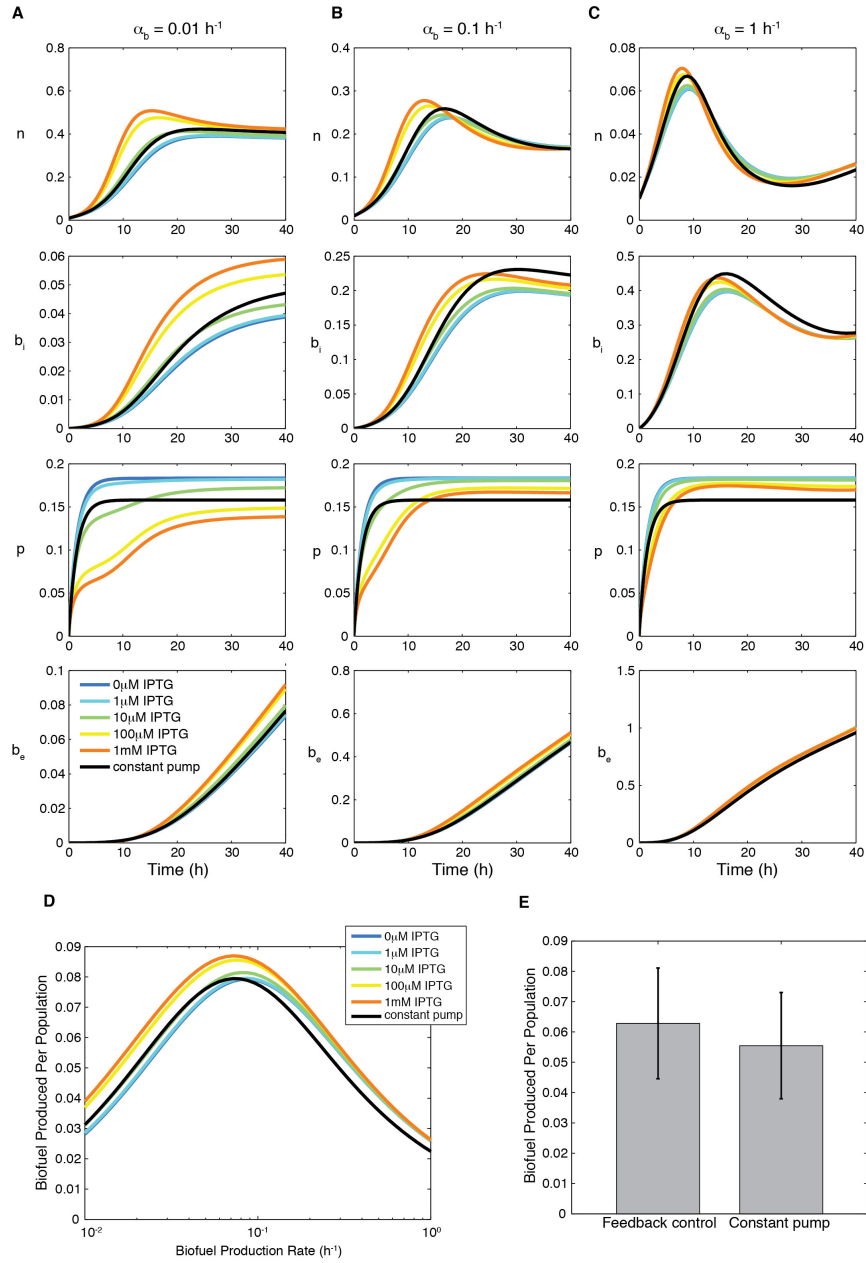production is more pronounced when a system is noisy.

Figure 3. Constant pump versus feedback control model using a biosensor. Transient behavior for growth n, intracellular biofuel b_i, pump expression p, and extracellular biofuel b_e for biofuel production rates α_b of (A) 0.01 h^{-1}, (B) 0.1 h^{-1}, and (C) 1 h^{-1}. Note the differences in y-axis scales. (D) Relative biofuel produced per population as a function of biofuel production rate. (E) Relative biofuel produced per population when the biofuel production rate is variable. Error bars show standard deviation.

2.3   Discussion

We present a model for a synthetic feedback control system to increase cell viability and biofuel production, quantify parametric sensitivity, and test the effect of variability in one of the model's key parameters. Our model implements a realistic mechanism of efflux pump control that utilizes a biosensor. The biosensor we chose represses efflux pump expression until it is deactivated by biofuel, which is a common type of regulation in bacterial transport systems [15, 31]. This regulation mechanism assures that efflux pumps are repressed until biofuel is present, which minimizes the negative effects of efflux pump overexpression while ensuring that their expression is initiated when needed [18, 41].

The feedback model we developed demonstrates that a small subset of model parameters can influence the system's behavior, but most have minor effects. The influential parameters relate to the amount of biofuel produced, efficiency of pump export, toxicity thresholds for efflux pump expression and biofuel produced, and growth rate. For the system presented, many of these terms are based on experimental values. However, these parameter values, and the subsequent behavior of the system may change significantly if the biofuel produced, efflux system, or biosensor is altered. By considering multiple parameters, we show that if one variable is altered, it is possible to negate a detrimental effect by appropriately varying another influential parameter. It would be interesting to test the same biosensor with different efflux pumps or hosts to study the tunability of the system.

Even when optimized for maximal production, the constant pump model consistently produced less extracellular biofuel than the feedback model. This is due to the feedback sensor's ability to delay pump expression until it is necessary, which minimizes the negative effects of pump expression by allowing cells to grow well early on, and reduces energy requirements within the cell so that more biofuel can be produced. This delay results in increased early biofuel production even if both models reach a similar steady state biofuel production level. The advantages of a feedback control system are apparent when there is variation in the biofuel production rate, as is likely to be the case in a production setting. Therefore, the feedback model would prove useful in real-life applications where variability and noise are typical. Additionally, any increase in microbial biofuel yield directly correlates to a reduction in the cost of biofuel. Even a modest increase in yield can contribute to a significant reduction in production costs.

There are several possible extensions to this work. For example, diffusion was omitted here for simplicity, but could be incorporated into a model using this system to control tolerance mechanisms. Additionally, simulating different biosensors or tolerance mechanisms would test the modularity of the system, as well as how much initial tuning is required each time a component is modified. Similarly, by altering the biofuel production rate and toxicity coefficient, the applicability of the sensor to various potential biofuels could be determined. Feedback control represents an important contribution to synthetic biology designs for optimizing biofuel yields and will be an important area for future experimental studies.

Chapter 3   Experimental Biosensor

3.1   Methods

3.1.1   Identify biofuel responsive sensor

We conducted a literature review and compiled a list of biosensors (Table 2) that respond to hydrocarbons and alcohols and would therefore be candidates for detectors of bio-gasoline, bio-diesel, and bio-jet fuel. The list is comprised of transcription factors that serve as activators and repressors and whose response to biofuel involves transcriptional regulation of a promoter.

We chose to focus on one prototypical biosensor for this study; MexR was selected because its associated efflux pump, MexAB-OprM, has been shown to improve tolerance to various types of biofuel and biofuel-related compounds [16, 17, 42]. Therefore, we hypothesize that MexR has a role in regulating this response and may respond to biofuels. MexR is a transcriptional repressor from *Pseudomonas aeruginosa* that controls the *mexAB* operon by binding to its promoter P_{mexA} [43]. If MexR does not directly detect the biofuel molecules, another possible mechanism for response is through the detection of oxidative stress. MexR is known to respond to oxidative stress and a recent paper showed that oxidative stress is induced when *E. coli* is exposed to butanol [44, 45]. Under oxidative stress, reactive oxygen species trigger a structural modification in MexR, which renders it incapable of binding to P_{mexA} [46]. Without the ability to bind, MexR is no longer able to repress P_{mexA}.

Table 2. List of potential biosensors. A list of biosensors shown to sense biofuel-like compounds or associated with biofuel tolerance mechanisms.

Biosensor	Substrate	Method of Regulation	Organism
TbuT [47]	2-methyl-2-butene, alkyl substituted benzene derivatives, toluene	Activator	*Ralstonia picketti* PK01
TtgV [48, 49]	mono and bicyclic aromatic compounds	Repressor	*Pseudomonas putida* DOT-T1E
TtgR [49-51]	anitbiotics, aromatic solvents, plant antimicrobials, toluene	Repressor	*Pseudomonas putida* DOT-T1E
TtgT [49]	styrene, benzonitrile	Repressor	*Pseudomonas putida* DOT-T1E
AcrR [45]	ethanol, NaCl, antibiotics, general stress	Repressor	*Escherichia coli*
MexR [43, 45]	antibiotics, oxidative stress	Repressor	*Pseudomonas aeruginosa*
Bmor [52]	carbon starvation, alcohol and aldehyde products of n-alkane oxidation, physiological substrates, primary alcohols(C2-C8)	Activator	*Pseudomonas butanovora*
XylR [53, 54]	toluene and toluene-like compounds	Activator	*Pseudomonas putida* mt-2, *Pseudomonas putida* KT22440
XylS [55]	Benzoate	Activator	*Pseudomonas putida* mt-2
SepR [56]	aromatic pollutants	Repressor	*Pseudomonas putida* F1
TbtR [57]	n-hexane, antibiotics	Repressor	*Pseudomonas stutzeri*
SrpS [58-60]	toluene, benzene	Repressor	*Pseudomonas putida* S12
AlkR [61]	alkanes (C>6)	Activator	*Acinetobactor* sp. Strain ADP1
AlkS [62-64]	alkanes (C6-C12), linear alkanes, branched alkanes	Activator	*Pseudomonas oleovorans*; *Pseudomonas putida* P1
TbmR [65]	toluene, benzene, chlorobenzene	Activator	*Burkholderia pickettii* PK01
IbpR [66]	Aromatics	Activator	*Pseudomonas putida* RE204

3.1.2 Design of biosensors, positive, and negative controls

All sensors use MexR as the biosensor and monitor its regulation over P_{mexA} using the fluorescent reporter protein *rfp*. When bound to P_{mexA}, MexR should repress transcription of *rfp*. MexR and P_{mexA} were amplified from *P. aeruginosa* PA01 genomic DNA by polymerase chain reaction. The entire intergenic region between the coding regions of *mexR* and *mexA* was used as P_{mexA}. The full sensors were cloned into BioBricks plasmid pBbA5k-RFP [67] (Fig. 4) using the Gibson Assembly Method [68], or derived from previously constructed sensors using mutagenesis, and then transformed

into *E. coli* MG1655 electro-competent cells via electroporation. Plasmid pBbA5k-RFP

is a medium copy plasmid that confers Kanamycin resistance to the host and features an

inducible promoter, lacUV5 (P_{Lac}). The controls are also variants of pBbA5k-RFP, were

constructed using similar methods, and transformed into *E. coli* MG1655. Finally, all
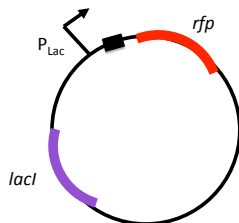
plasmids were confirmed by sequencing.

Figure 4. pBbA5k-RFP. BioBricks plasmid used for construction of experimental biosensors. The black
square represents the ribosome binding site.

Biosensor S1

Biosensor S1, which is shown in Figure 5A, places *mexR* under the control of P_{lac},

which enables *mexR* expression to be induced by adding isopropyl β-D-1-

thiogalactopyranoside (IPTG) to the culture. P_{mexA} follows *mexR*, but is separated by a

terminator to prevent read-through transcription. The biosensor components are inserted

into pBbA5k-RFP between P_{lac} and *rfp*.

Biosensor S2

Biosensor S2 (Fig. 5B) is a variation of Biosensor S1. It has the same plasmid

construction, but with the terminator removed via mutagenesis. Terminators work by

forming a hairpin structure in the newly formed mRNA strand, which disrupts further

transcription of genes downstream of the terminator. We hypothesized that this hairpin

structure may be restricting gene expression on the plasmid in general instead of only limiting transcription of *rfp* when *mexR* was induced by IPTG. More specifically, the hairpin structure may be preventing RNA polymerase from binding to adjacent P$_{mexA}$ and therefore inhibiting expression of rfp under all conditions.
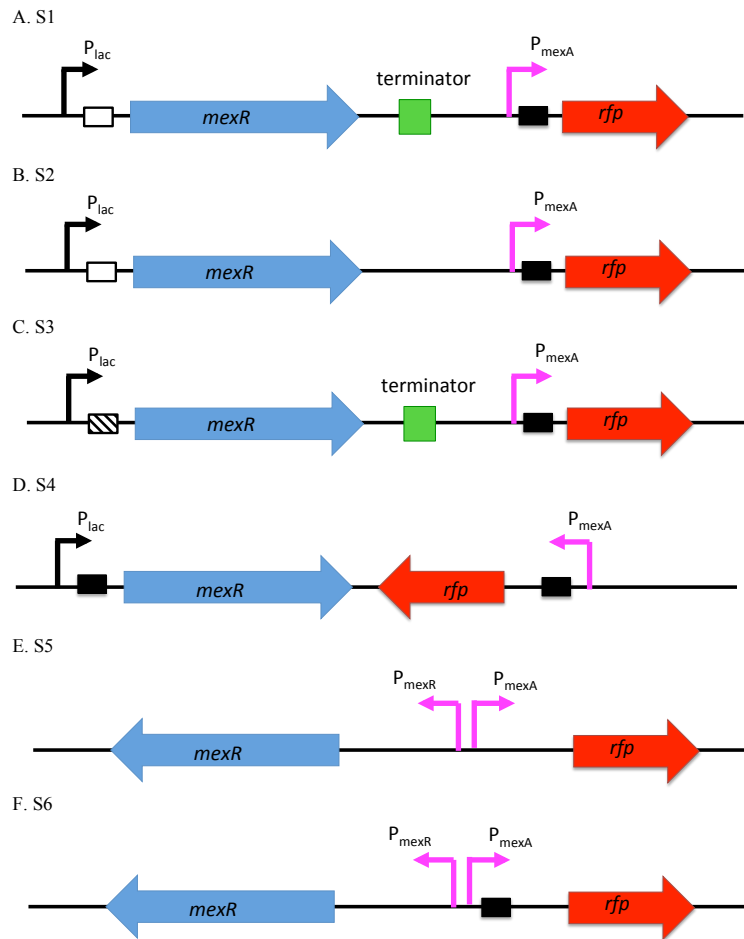

Figure 5. Schematic of Biosensor constructs. (A) S1. (B) S2. (C) S3. (D) S4. (E) S5. (F) S6. Note that the box in front of *rfp* or mexR represents the RBS: if black, the original RBS from pBbA5k-RFP is used; if white, an RBS from another plasmid is used; if textured, 0031 is used; if absent, no additional RBS was used. All constructs additionally use the native RBS associated with P$_{mexA}$.

Biosensor S3

Biosensor S3 (Fig. 5C) differs from Biosensor S1 (Fig. 5A) in the ribosome binding site for *mexR*, which has been replaced with BBa_B0031 [11]. We hypothesized

that MexR was too prevalent in the system based on the low fluorescence exhibited by S1 under all conditions. The low fluorescence values even when *mexR* was not induced indicate that *mexR* was transcribed and translated too readily. One possible cause of this result is that the ribosome binding site (RBS) for *mexR* is too strong. A known weak ribosome binding site, BBa_B0031, was substituted for the existing one using mutagenesis.

Bisosensor S4

Biosensor S4 is an inverted variant of Biosensor S1. As is seen in Figure 5D, the orientations of *rfp* and P_{mex} are rotated and the terminator is removed. To prevent read through transcription from occurring, *rfp* and its promoter, P_{mexA}, were rotated so that they faced *mexR* rather than following *mexR*. In this way, if transcription continued, the transcript would not contain a viable open reading frame. S4 was assembled from P1 (Fig. 7A) and the negative control (Fig. 6). P_{mexA} and *rfp* were amplified from P1 and P_{lac}, *mexR*, and the remaining vector were amplified from the negative control plasmid. This construct also provides *mexR* and *rfp* with the same RBS.

Biosensor S5

Biosensor S5 (Fig. 5E) implements the native configuration of *mexR* and P_{mexA} from *P. aeruginosa* PA01. P_{mexA} and *mexR* were amplified from *P. aeruginosa* genomic DNA as a continuous piece of DNA rather than as individual parts. Biosensor S5 makes use of P_{mexR}, which is included in the intergenic region between *mexR* and *mexA*. In Biosensors S1 through S4, P_{mexR} is oriented so that it does not control *mexR*. P_{mexR} is

25

oriented in the opposite direction of P_{mexA} with overlapping regions and is also controlled by MexR. This construct was then cloned into the same plasmid as the previous sensors so that P_{mexA} controls *rfp* [68]. The native sensor was built to better understand MexR's control over P_{mexA} under our experimental conditions. It is simpler than Biosensor S1 because *mexR* expression is not inducible. Instead, *mexR* autoregulates its own transcription, which should control the MexR levels within *E. coli* MG1655 as it does natively in *P. aeruginosa*.

Biosensor S6

Biosensor S6 (Fig. 5F) is an adapted form of Biosensor S5. The *rfp* ribosome binding site from Biosensor S1 is added to the region between P_{mexA} and *rfp*. This insertion was accomplished by amplifying the vector (plasmid pBbA5k-RFP) with the RBS and cloning P_{mexA}, P_{mexR}, and *mexR* as described above for Biosensor S5. The additional RBS was added to boost expression of *rfp* because fluorescence in Biosensor S5 was low overall. This should have the effect of amplifying the effects of MexR's control.
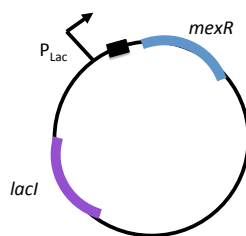

Figure 6. Negative control plasmid pBbA5k-mexR (N).

Negative control: N

The negative control (Fig. 6) replaces *rfp* with *mexR* on plasmid pBbA5k-RFP.

Positive controls

A positive control was assembled for S1 and its variants (S2 and S3), S4, S5, and S6. Schematics of all positive control plasmids are shown in Figure 7. The positive control for S1, S2, and S3 is P1 (Fig. 7A), which removes P_{lac} from pBbA5k-rfp and inserts P_{mexA} to control *rfp*. The positive control plasmid for S4, P2 (Fig. 7B), was constructed by removing P_{lac} and *mexR* from S4. P3 (Fig. 7C) and P4 (Fig. 7D), the positive controls for S5 and S6 respectively, removed *mexR*, P_{lac}, and *lacI* from S5 and S6 using mutagenesis. P4 also served as an alternative positive control for sensors S1, S2, and S3.
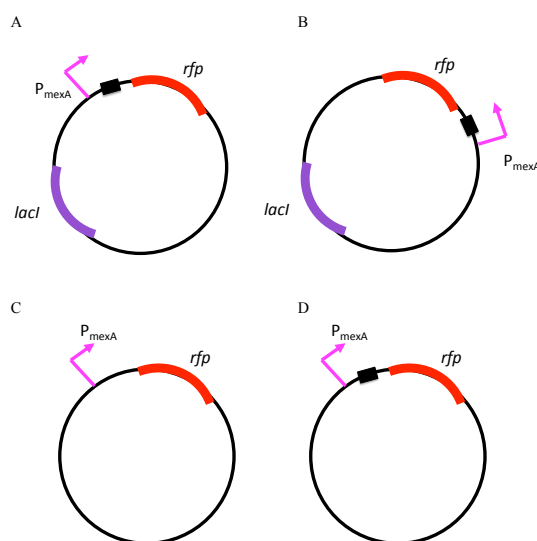
Figure 7. Positive control plasmids. (A) P1, the positive control for biosensors S1, S2, and S3. (B) P2, the positive control for biosensor S4. (C) P3, the positive control for biosensor S5. (D) P4, the positive control for biosensor S6.

3.1.3   Characterize biosensors

Five milliliter cultures of LB from an individual colony were grown shaking at 200rpm and 37°C overnight with a final concentration of 30μg/mL kanamycin to ensure retention of the plasmid. Overnight cultures were then diluted 1:100 into fresh M9 (for

27

200mL M9: 40mL 5x M9 salts, 400μL 1M MgSO$_4$, 4mL 20% glucose, 20μL 1M CaCl$_2$, 20μL 0.5% Thiamine, 4mL 5% casamino acids, 160mL de-ionized H$_2$0) with kanamycin and the appropriate stressor and transferred to a 24 well plate. Biofuel stressors include butanol and pinene and replicates were derived from a single overnight culture. Additionally, IPTG was added to the culture at a final concentration of 100μM for induced conditions. The new cultures were grown in a Synergy H1m plate reader (BioTek Instruments, Inc.) at 37°C measuring fluorescence (excitation: 551nm, emission: 590nm) and optical density (absorbance at 600nm) every 10 minutes for 16 hours.

3.1.4   Positive control experiments

In order to confirm the generation of reactive oxygen species (ROS) in the culture when butanol was present, we used carboxy-H$_2$DCFDA (carboxy-2', 7'-dichlorodihydrofluorescein diacetate) as a ROS indicator as in Rutherford *et al.*, 2009 [44]. Carboxy-H$_2$DCFDA (Life Technologies Corporation) is a molecular probe that turns green in the presence of ROS in live cells.   We prepared cultures of *E. coli* possessing biosensor S1 as described in the previous section, diluted and stressed them with butanol for an additional overnight, and finally diluted the cultures 1:50 into fresh M9 with all stressors. Cultures were then grown to exponential phase, at which point 57.2uL 250μM carboxy-H$_2$DCFDA solution was added, and fluorescence (excitation: 495, emission: 529) and optical density (600nm) were measured every 5 minutes for 45 minutes in the plate reader at 37°C. Tert-butyl hydroperoxide (TBHP), a known ROS generator, was used as the positive control for this assay. It was added to control cultures following the dilution from stressed overnight growth.

Tetracycline, a bacteriostatic antibiotic targeting the 30S ribosomal subunit, is exported through *mexAB-oprM.* Since MexR responds to tetracycline, it was used in another positive control experiment [46, 69]. Tetracycline was added to cultures following dilution into fresh M9 and any fluorescence from RFP was detected using the Synergy H1m plate reader as cells continued overnight growth at 37°C.

3.1.5 Data analysis

The fluorescence, optical density, and normalized fluorescence, which is the raw fluorescence normalized by the optical density to account for the number of cells in the culture, were all measured. All analyses were performed using custom software developed using MatLab (The Mathworks, Inc.). To avoid measurement noise, the last 10 time points were averaged for raw fluorescence and normalized fluorescence. Finally, these averages for biological replicates were then averaged together.

3.2   Results

3.2.1   Biosensor response to butanol

The response to butanol was considered first because it is known to induce oxidative stress in *E. coli,* which would cause a change in MexR's activity [44, 46]. The biosensor should respond to IPTG by initiating *mexR* expression, which will bind to P_{mexA} and inhibit *rfp* expression. When biofuel is added to the culture, the induction of oxidative stress should alter the structure of MexR so that it is no longer able to bind and repress P_{mexA}. Therefore, we expect fluorescence to be higher when the concentration of

IPTG is low and when the concentration of biofuel is high (Fig. 8A). We used butanol as an initial biofuel to test the sensor. To determine the appropriate concentrations of butanol to use, we performed a butanol toxicity experiment. As shown in Figure 9, 0.6% butanol inhibited growth significantly. A characteristic experimental result for S1 with butanol is shown in Figure 8B. By comparing Figure 8A and 8B, we show that the biosensor behaves as expected. However, the dynamic range of *rfp* expression is small, which is indicated by the range of AFU.
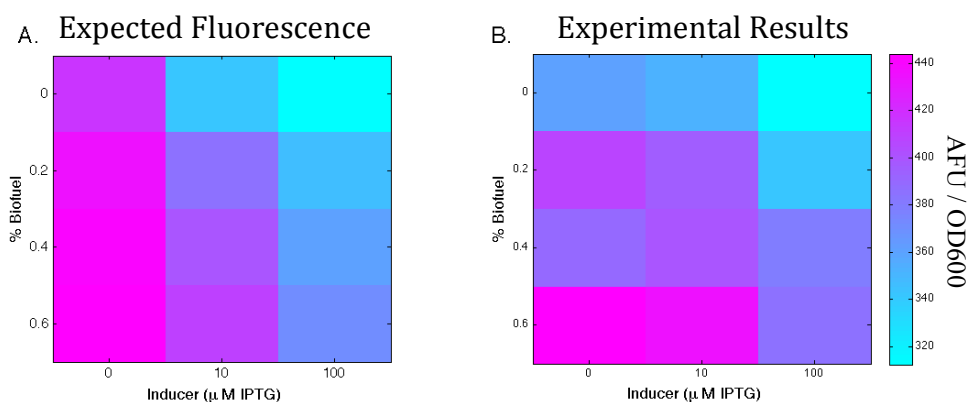
Figure 8. (A) Expected fluorescence and (B) Experimental fluorescence (arbitrary fluorescence units) of S1 cultures after entry into stationary phase. The fluorescence shown is an average of three biological replicates and normalized by optical density. The biofuel used in these experiments is butanol.
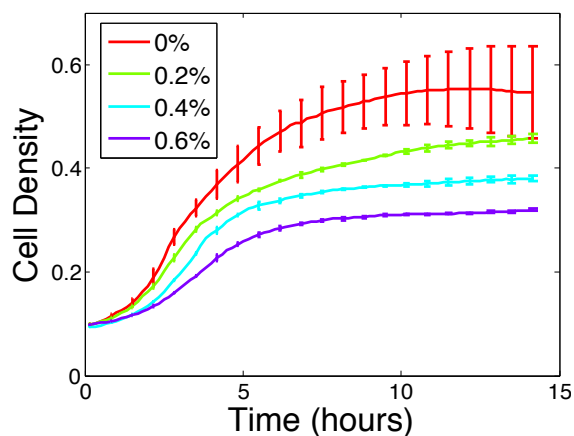
Figure 9. Butanol toxicity experiment. The error bars show standard deviation for three biological replicates.

To investigate the full range of fluorescence to be expected, positive (P1) and negative (N) controls were constructed. Biosensor S1 is tested with butanol and compared to the positive and negative controls in Figure 10. The biosensor shows a similar trend to that observed earlier (Fig. 8): Fluorescence decreases when IPTG is increased from 0 to 100μM for 0% butanol conditions and for both IPTG conditions when butanol is added to the system (Fig. 10A). However, the change in fluorescence for S1 is very small in comparison to difference between the positive control and the negative control (Fig. 10B).

A

B
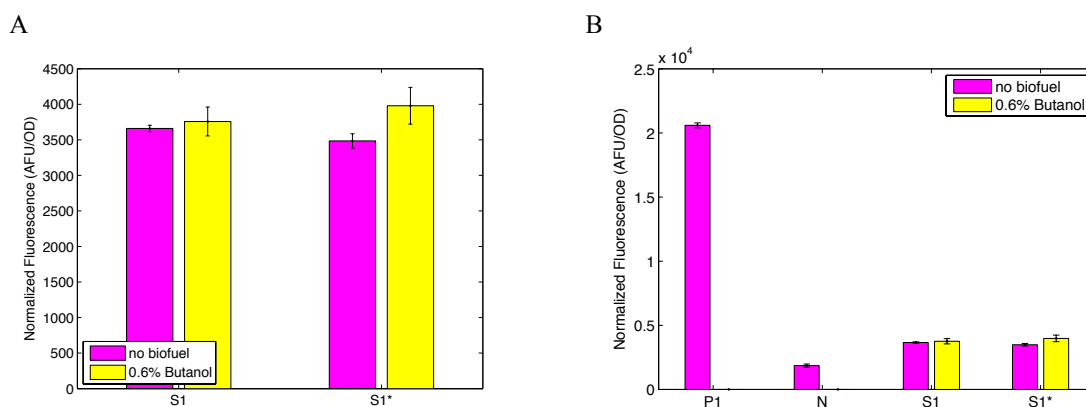
Figure 10. Fluorescence of Biosensor S1 grown with butanol. (A) Biosensor S1 only. (B) Biosensor S1 and controls: Negative control (N) is pBbA5k-mexR and positive control is P1. (*) denotes that the sensor is induced with 100μM IPTG. The error bars shown represent the standard deviation of three biological replicates.

We hypothesized that too much MexR was present in the system, which prevented *rfp* from being expressed. If this is the case, enough biofuel to deactivate MexR could not be added to the system without greatly inhibiting growth. Alternatively, the terminator may be interfering with activation of the *rfp* promoter P_{mexA}. To explore these hypotheses, Biosensors S2, which removed the terminator from S1, and S3, which

implemented a weaker *mexR* RBS than S1, were developed and tested. The responses of S2 and S3 to butanol are shown in Figure 11A and Figure 11B respectively. Figure 11A shows that adding IPTG to S2 increases fluorescence, which is the opposite of what was expected. This is observed by comparing S2 to S2*. This curious result may be caused by initiation of transcription of *rfp* from activation of the *mexR* promoter P_{lac}, known as read-through transcription. However, the trend of increasing fluorescence as biofuel is added to the system is preserved when the sensor is induced with IPTG. Overall, although removing the terminator does increase the range of expression for S2 in comparison to S1 (Fig. 10), the trend in fluorescence is not helpful for use in a potential feedback system because fluorescence increases dramatically when *mexR* is induced (Fig. 11A). Increasing MexR should increase repression of *rfp,* which should decrease fluorescence, particularly when biofuel is not present.

Figure 11B shows the effect of butanol on S3. Fluorescence is lowered when IPTG is added to the system when butanol is absent. Fluorescence is also increased when butanol is added to the system for both induced and uninduced systems. However, S3 exhibits a lower maximal normalized fluorescence than S1 (Fig. 10), which indicates that the strength of the *mexR* RBS is not preventing *rfp* from reaching maximal expression.

Biosensor S4, which orients *rfp* and P_{mexA} in the opposite direction so that read-through transcription is not possible, was also tested with butanol stress (Fig. 11C). S4 displays increased fluorescence in response to 0.6% butanol, but only a slight increase for 0.3% butanol. Additionally, S4 exhibits a dynamic range of approximately 3000 AFU / OD. This trend of increasing fluorescence indicates that the fluorescence may continue

to increase if the concentration of butanol in the system was also increased, however

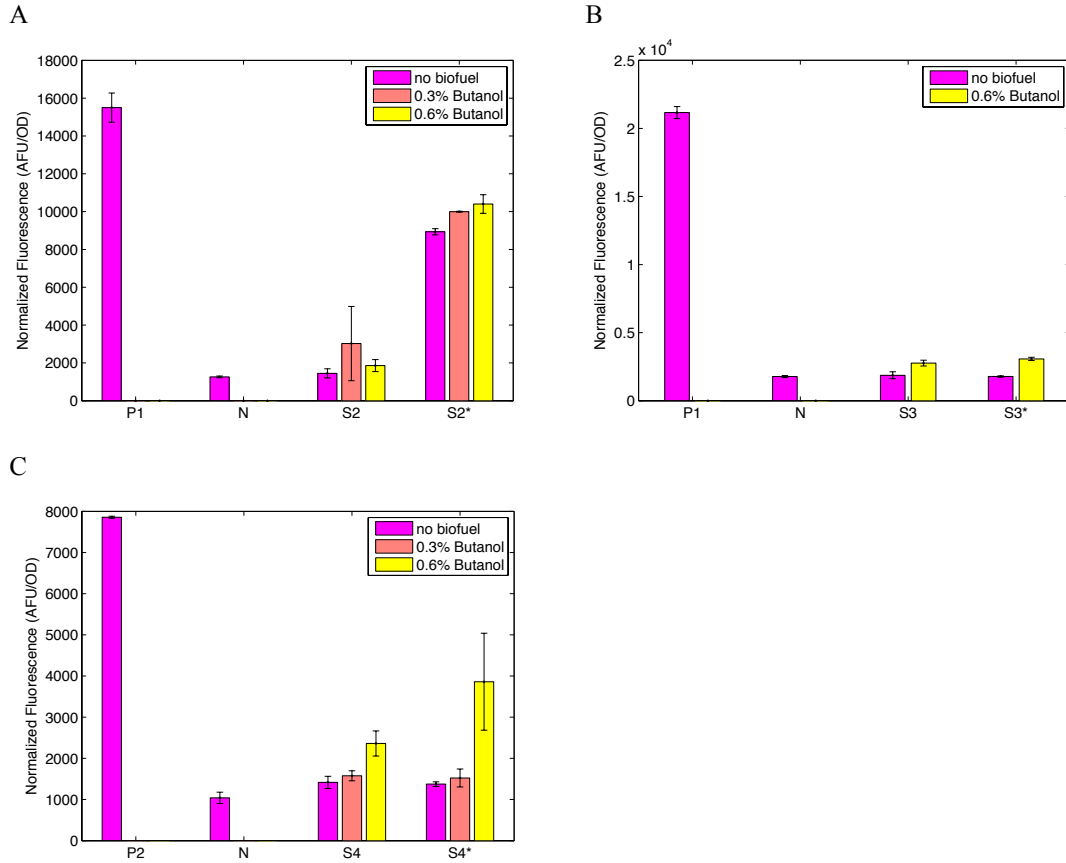0.6% butanol presents a near-toxic level.

Figure 11. Response of (A) Biosensor S2, (B) Biosensor S3, and (C) Biosensor S4 to butnaol. Negative control (N) is pBbA5k-mexR for all, positive control is P1 for (A) and (B) and P2 for (C). (*) denotes that the sensor is induced with 100μM IPTG. Note that error bars shown for 0.3% butanol in (A) are based on the standard deviation of two biological replicates while all other error bars represent the standard deviation of three biological replicates.

Finally, the native orientation of the sensor was considered. S5 places *mexR*

under P_{mexR} control and removes P_{lac} from the plasmid backbone. S6 is identical to S5,

but with the *rfp* RBS from the original vector included in addition to the native RBS.

Figure 12A shows S5 and S6 after growth overnight with butanol stress. The higher

fluorescence displayed by S6 for each butanol concentration indicates that the additional

rfp RBS increases transcription of *rfp*. However, the range of expression of both S5 and

S6 is similar. Therefore, the additional RBS increases overall expression rather than

amplifying a response to butanol. This increased fluorescence is also seen in the positive

controls for S5 and S6 (Fig. 12B). P4, the positive control for S6 fluoresces much more

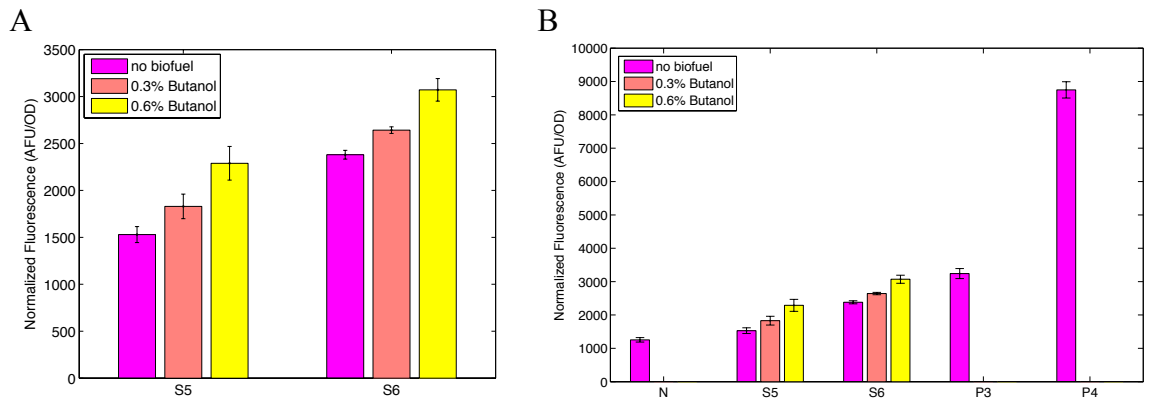highly than P3, the positive control for S5.

Figure 12. Fluorescence response of Bisoesnor S5 and Biosensor S6 to butanol stress. (A) Biosensor S5 and S6 only. (B) Biosensors S5 and S6 with N (negative control) and P3 (positive control for S5) and P4 (positive control for S6). The error bars for N represent the standard deviation for two biological replicates, the error bars for P3 and P4 show the standard deviation for four biological replicates, and all other error bars show the standard deviation for three biological replicates.

The positive controls show the maximum fluorescence that can be expected for a

given sensor. Similarly, the negative control shows the background fluorescence, or

autofluorescence, that is exhibited by cells naturally. Furthermore, when compared to the

sensor's performance, the controls show if the sensor is functioning throughout the

expected range. The positive control plasmids are compared in Figure 13. P1, the

original positive control, displays the highest fluorescence and P3, the positive control for

the native construct S5, displays the lowest fluorescence. This low fluorescence may be

due to the absence of the additional *rfp* RBS. S5 fluoresces almost as highly as its

positive control P3. However, S5 may not be a viable sensor because its dynamic range,

indicated by fluorescence, is small. P2, the positive control for S4, exhibits a lower

fluorescence than P1. This result makes S4 more practical in comparison to the other

sensors because it exhibits a larger range of fluorescence than the other sensors and

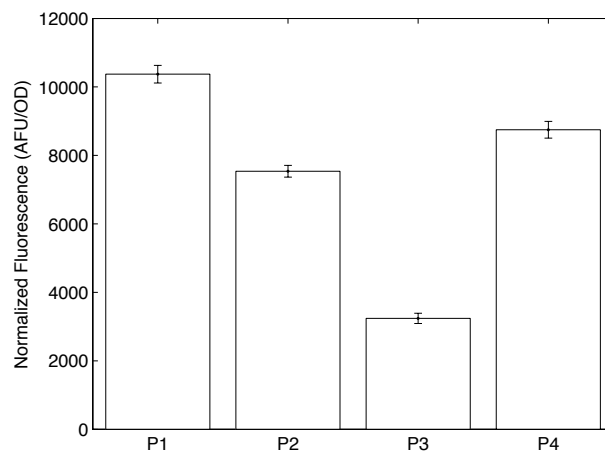reaches about half of the maximum fluorescence possible as predicted by P2.

Figure 13. Normalized fluorescence for all positive control plasmids expressed in *E. coli*. Error bars show
standard deviation of four biological replicates.

3.2.3   Biosensor response to pinene

Pinene, a potential replacement for jet-fuel, was considered. Figure 14 shows

how the top four sensors (S1, S2, S5, and S6) responded to a 2% concentration of pinene.

S1 and S4 do not show a positive response to pinene. S5 and S6 show a positive

correlation between pinene added to the system and fluorescence with S6 continually

fluorescing more highly than S5. Overall, none of the sensors demonstrate a strong
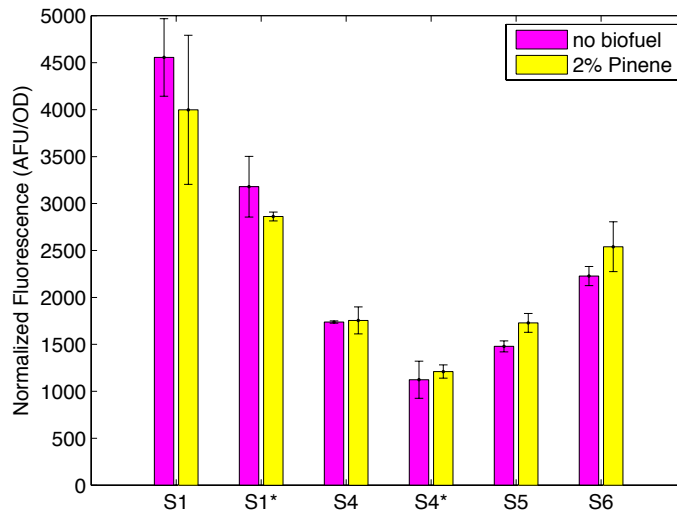
response to pinene.

Figure 14. Biosensor response to pinene. Normalized fluorescence for sensors S1, S4, S5, and S6 based on 2 biological replicates is shown. (*) denotes that the sensor is induced with 100μM IPTG. The error bars represent the standard deviation for replicates.

3.2.4 Biosensor response to tetracycline

The top four sensors (S1, S2, S5, and S6) were tested with tetracycline, a known export of MexAB-OprM (Fig. 15). S1 exhibits the strongest trend in increasing normalized fluorescence in response to tetracycline. S4 responds better when uninduced than when induced with IPTG, but displays a general increase in fluorescence for both states. S5 shows a slight positive trend in fluorescence corresponding to increased tetracycline. However, tetracycline does not elicit a clear response from S6. The tetracycline assay shows that sensors S1 and S4 are capable of generating a large response range if exposed to the proper compound in the proper concentration. Additionally, if a small dynamic range is needed, S5 demonstrates a consistent trend.
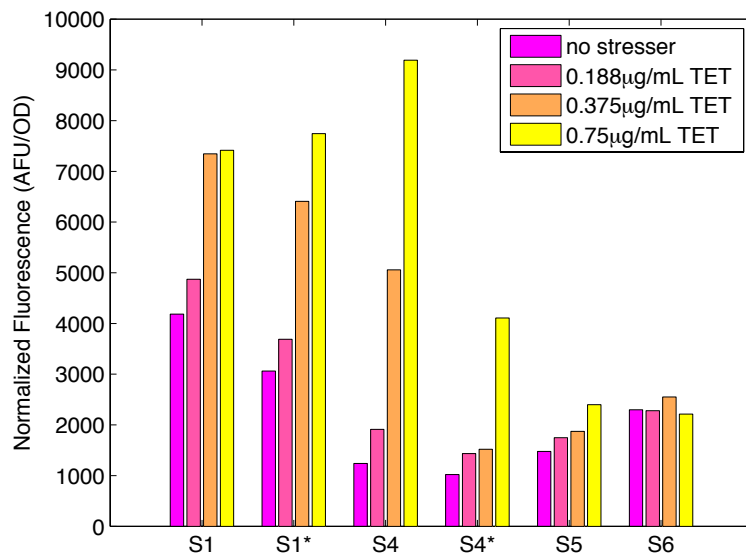
Figure 15. Biosensor response to Tetracycline. (*) denotes that the sensor is induced with 100μM IPTG.

3.2.5 ROS assay

Molecular probe carboxy-H$_2$DCFDA was used to detect the presence of ROS in experimental cultures. Figure 16 shows that fluorescence increases for higher concentrations of butanol. Although the fluorescence does not reach levels as high as the positive control, 0.9% butanol does produce a considerable increase in fluorescence compared to lower concentrations of butanol. Therefore, butanol does contribute to ROS in the system, but higher concentrations of butanol may be necessary to sufficiently deactivate MexR and induce expression of *rfp*. Increasing the concentration of butanol poses an experimental problem because it would stress cells and greatly inhibit growth.
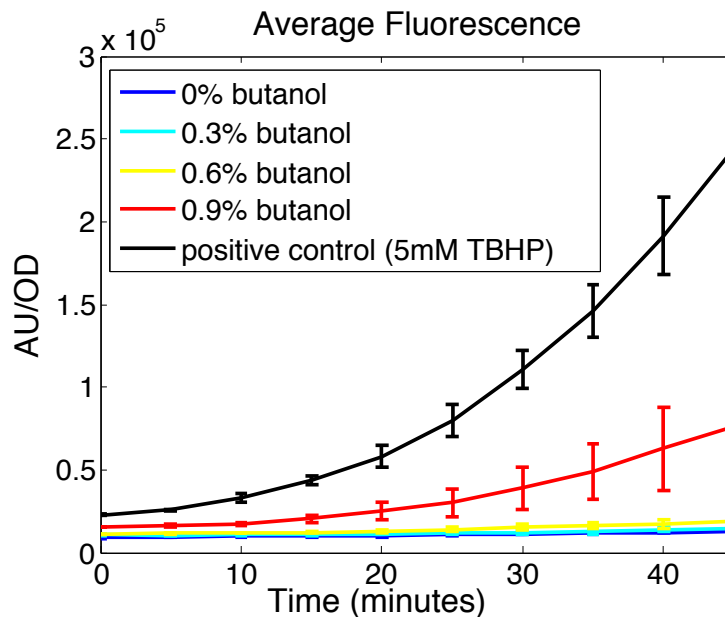
Figure 16. Reactive oxygen species generation in *E. coli*. Fluorescence results from molecular probe carboxy-H$_2$DCFDA that fluoresces when reactive oxygen is detected. TBHP serves as the positive control. The error bars show the standard deviation for three biological replicates.

3.3   Discussion

We selected MexR, a transcriptional repressor, as the sensor because its associated efflux pump successfully improves tolerance to many existing fuels and biofuels in development [16, 42]. Therefore, MexR, as the regulator for this export, may be also be responsive to compounds present in fuel.

We constructed six whole cell biosensors to test the effectiveness of MexR as a sensor for various types of biofuel. Each sensor uses MexR in a slightly different way, but all used P$_{mexA}$, which is controlled by MexR, to regulate expression of *rfp*. The sensors were tested with potential biofuels, including butanol and pinene, as well as tetracycline, a known export of MexAB-OprM. Sensors S4 and S5 performed the best across all tests. The range of expected expression from an operon under MexR control

38

varies across the literature from a 1.6-fold increase [38] to a 7- fold increase [39]. Neither Biosensor S4 or S5 approached a 7-fold increase, but they displayed at least a 1.5-fold change in fluorescence between the unstressed case (0% butanol) and 0.6% butanol. Biosensor S5 incorporates the native orientation and control for *mexR*. Although its dynamic range is not very large (1.5-fold change for 0% butanol to 0.6% butanol), its fluorescence is correlated to increased concentrations of butanol (Fig. 12), pinene (Fig. 14), and tetracycline (Fig. 15). Biosensor S4, which utilizes inducible *mexR* expression, displays a broader range of *rfp* expression for butanol (Fig. 11C) and tetracycline (Fig. 15), but does not respond to pinene (Fig. 14). S4 displayed a 1.7-fold change in fluorescence when the concentration of butanol was increased from 0 to 0.6% for uninduced conditions and a fold change of 2.8 for induced conditions. Therefore, S5 may be applicable if a small change in expression of a tolerance mechanism is needed and S4 may be useful when larger alterations in expression are necessary. For example, a small change in expression of an enzyme that increases tolerance may elicit a significant change in survival while a larger change in efflux pump expression may be needed to increase survival. It may even be possible to use these biosensors or similar ones in combination to control multiple tolerance mechanisms. Alternatively, another sensor could be selected from Table 2 for use in a synthetic feedback loop.

We have shown that it is possible to build a biosensor with MexR that responds to biofuel by fluorescing. However, both S4 and S5 require further characterization and development before they could be applied to regulating a tolerance mechanism. One potential method for improvement would be to utilize MexR's binding sites in a well-studied promoter as in Zhang et al., 2012 [28]. Another would be to use codon

optimization to ensure that *mexR* is expressed properly in the *E. coli*, which is a less GC

rich organism than *P. aeruginosa*. *E. coli* genomic DNA is about 51% GC [70] while the

mexR and P_{mexA} regions of *P. aeruginosa* are 56.7% GC. This difference in GC content

can lead to a deficiency in the proper machinery to translate RNA into protein. This

deficiency can be corrected by increasing expression of relevant t_{RNA}s or altering the

heterologously expressed genes [71, 72]. Additionally, the sensors should be tested with

other potential biofuels and more extensively tested with butanol and pinene. Later, it

would be useful to examine their utility as a sensor in a feedback loop by replacing *rfp*

with a tolerance mechanism. Furthermore, this completed sensor should then be

expressed in a fuel production host.   A biofuel responsive controller for tolerance

mechanisms may prove useful in improving biofuel yields by balancing the detrimental

effects of biofuel with the negative effects of overexpressing tolerance mechanisms.

Chapter 4   Increasing Tolerance with *cti*

4.1   Methods

4.1.1   Plasmid construction

Cis-to-*trans* isomerase, *cti,* was amplified from *Pseudomonas putida* KT 2440 and cloned into BioBricks plasmid pBbA5a-rfp in the place of *rfp* using restriction sites to form pBbA5a-cti. Plasmid pBbA5a-cti places *cti* under control of the lacUV5 promoter, P_{lac}, which is inducible by IPTG. The plasmid was then transformed into *E. coli* MG1655 and confirmed by sequencing. Cis-to-*trans* isomerase was expressed in *E. coli* because *E. coli* lacks its own version of *cti* [73]. Therefore *cti* expressed from pBbA5a-cti did not compete with a native *cti* gene on the chromosome and we were able to control the level of *cti* expression in the bacterium.

4.1.2   Tolerance experiments

To determine if the expression of *cti* confers increased tolerance to E. *coli* MG1655, 5mL LB cultures were grown in a shaking incubator at 200rpm and 37°C overnight with 5μL 100mg/mL ampicillin. They were then diluted 1:100 into selective M9 with ampicillin and stressed with ethanol, octanol, or butanol. In some cases, *cti* expression was further induced with IPTG. This culture was grown overnight at 37°C or 30°C. Although *E. coli* grows best at 37°C, *cti* is most commonly present in organisms that inhabit colder climates and it was previously established that colder temperatures are needed for enhanced *cti* expression [19]. After 12-16 hours of growth, the optical density at 600nm was measured using the NanoDrop 2000 Spectrophotometer (Thermo Fisher

Scientific Inc.) and compared to the optical density of *E. coli* MG1655 cultures grown
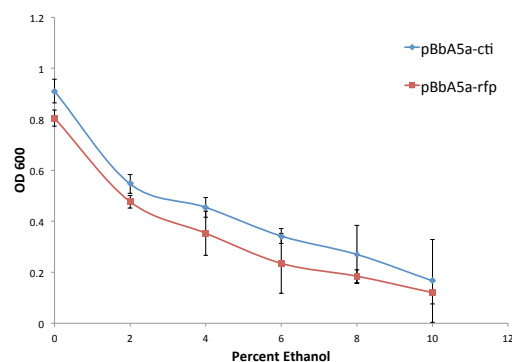
under the same conditions.

4.2 Results

4.2.1 Tolerance to ethanol

A.   Growth with Ethanol at 37°C   B.   Growth with Ethanol at 30°C
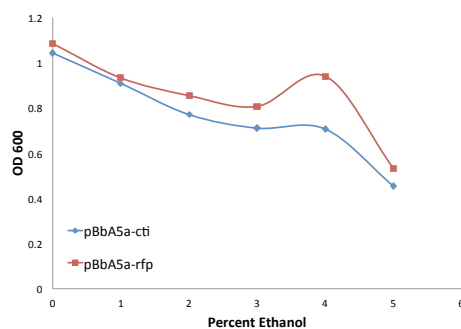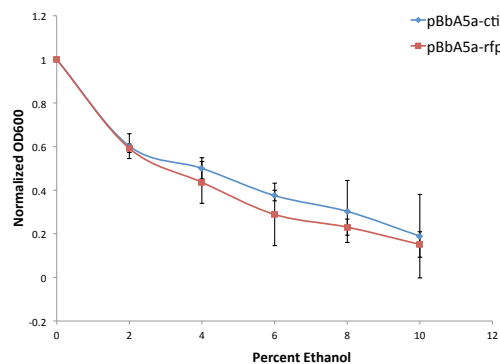
C.   Growth with Ethanol at 30°C

Figure 17. Overnight growth with ethanol stress. (A) Optical density for growth at 37°C . (B) Optical density and (C) normalized optical density at 30°C. The optical density after overnight growth is compared for cells possessing pBbA5a-cti (blue) and pBbA5a-rfp (red). Note that *cti* was not induced for either experiment and that (B) and (C) represent the same data. The error bars shown in (B) and (C) represent the standard deviation of three biological replicates.

Overnight growth for cells possessing pBbA5a-cti is compared to those

possessing pBbA5a-rfp in Figure 17. *Cis-trans*-isomerization does not increase tolerance

and survival in ethanol stress at 37°C in comparison to the control (pBbA5a-rfp) as

evidenced by the lower optical density reached by cells expressing *cti* (Fig. 17A). Figure

17B shows that pBbA5a-cti may give cells a slight advantage at 30°C. Additionally, the

normalized optical density (Fig. 17C) shows that this improved growth is not an artifact

of the differing optical densities reached. However, growth is not significantly different

for most ethanol concentrations between cells possessing and not possessing *cti*.

Although the improved survival observed for pBbA5a-cti at 30°C coincides with

previous research [19], both types of cells reached higher optical densities at 37°C.

Collectively, Figure 17 shows that even uninduced levels of Cti impact growth with Cti

slightly inhibiting growth at 37°C and slightly improving growth at 30°C.
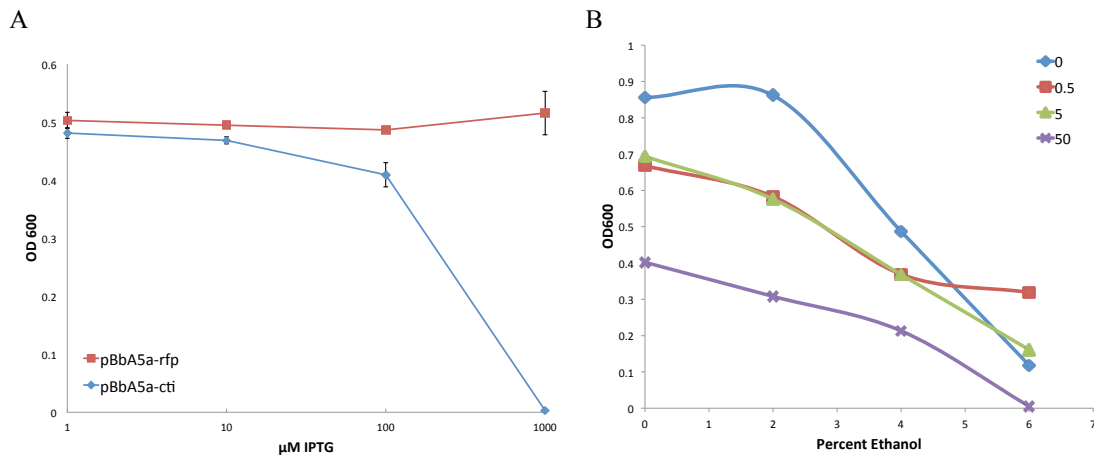
Figure 18. Effect of varying IPTG on ethanol tolerance. (A) Effect of increasing IPTG at 4% ethanol for cells expressing pBbA5a-cti (blue) and pBbA5a-rfp (red). (B) Effect of varying IPTG at various ethanol concentrations for pBbA5a-cti hosts. The legend represents IPTG concentrations in μM. Both experiments were conducted at 30°C. The error bars shown in (A) represent the standard deviation for three biological replicates.

To further consider the effects of Cti, IPTG, which induces expression of *cti,* was

added to cultures. Figure 18A shows that increasing expression of *cti* does not severely

affect growth until it is heavily induced (1000 μM). Furthermore, Figure 18B shows that

lower levels of *cti* induction may aid growth at higher ethanol concentrations. However,

it is clear that Cti may be detrimental to cell growth when it is not needed to improve tolerance, which is best exemplified by the difference in optical density between 0μM IPTG and 50μM IPTG for 0% ethanol in Figure 18B.

4.2.2   Tolerance to other potential fuels

Butanol (Fig 19A) and octanol (Fig. 19B) were also considered as possible biofuels. Although they are both toxic to *E. coli,* which is observed in the decreasing optical density for increasing concentrations of solvent, there were no indications that Cti may improve tolerance to either solvent based on overnight growth experiments (Fig. 19).
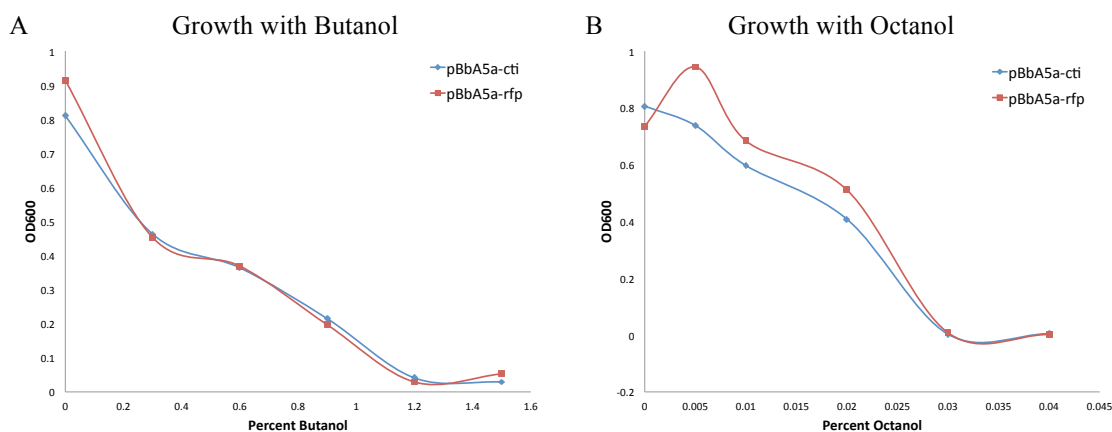
Figure 19. Overnight growth with (A) butanol stress and (B) octanol stress. Optical density following overnight growth for cells possessing pBbA5a-cti (blue) and pBbA5a-rfp (red) at 30°C.

4.3   Discussion

Cis-to-*trans* isomerase is an enzyme that helps convert *cis* fatty acids in the membrane to *trans* fatty acids. It is used by several *Pseudomonas* species in response to the presence of harmful solvents and aromatics that increase membrane fluidity. Increasing the ratio of *trans* fatty acids to *cis* fatty acids increases membrane rigidity, which is believed to counteract the effects of these solvents [15, 19, 20].

Cis-to-*trans* isomerase has recently been heterologously expressed in *E. coli* and shown to increase the ratio of *cis* to *trans* fatty acids in the membrane, particularly in the presence of ethanol [19]. Our results show that Cti may increase tolerance to ethanol at 30°C (Fig. 17B-C), but does not confer any added benefits for octanol (Fig. 19B) or butanol (Fig. 19A) exposure. Additionally, we have shown that heavily inducing *cti* can have negative effects on the growth of *E. coli*. Therefore, it is essential that the optimal level of *cti* expression be determined to further study its effects on tolerance to organic solvents. It may be helpful to consider the ratio of *trans* to *cis* fatty acids generated by expressing *cti* on plasmid pBbA5a-cti. This analysis would help compare the results we have observed with growth to changes in membrane composition observed in other studies [19].

Although Cti showed limited utility in our studies, it may be useful to express *cti* in combination with another tolerance mechanism. Cti is fast-acting [20], but we have shown that it may tax the cell when heightened expression is maintained (Fig. 18). Therefore, Cti could provide initial tolerance to biofuel and thus enable cells to induce a long-term mechanism that may require significant time to establish. The utility of Cti as a secondary tolerance mechanism could be initially explored by incorporating *cti* expression into the mathematical model described in Chapter 2. This addition may be accomplished by altering the biofuel toxicity coefficient in the growth equation (n) to reflect the decrease in toxicity observed when *cti* is expressed.

Chapter 5   Conclusions

In this thesis, we explored mechanisms for improving biofuel tolerance and export in an engineered host. First, we tested the utility of a synthetic feedback loop that incorporates a biosensor in improving growth and biofuel yields in a microbial production host. We identified several transcription factors that are sensitive to biofuel-like compounds, cellular responses to biofuel, or biofuels directly, which could serve as the biosensor in the controller system and selected a prototypical example, MexR, for further study.

We simulated this feedback control of an efflux pump operon with MexR as the biosensor and found that this system improved microbial fuel production in comparison to constant (no feedback) control. The feedback system effectively balanced the toxicity of biofuel with the detrimental effects of unnecessary efflux pump expression. This outcome provides further motivation for continued development of an effective biosensor system to be experimentally incorporated into a synthetic feedback loop.

To further study the effectiveness of MexR as a biosensor, we built six variants of the biosensor and tested them experimentally; two of these constructs consistently responded to butanol. Although this functionality is promising, the biosensor requires further optimization and characterization before it could be integrated into a feedback loop.

Cis to *trans* isomerase was also considered as a possible tolerance mechanism. However, we determined that Cti did not significantly improve survival in biofuel

conditions and was sensitive to temperature, induction levels, and the specific biofuel tested.

This study provides two biofuel-responsive sensors that implement MexR as well as an index of potential biosensors for future experimental constructs. Addditionally, we present a working mathematical model that can be adapted to investigate additional tolerance mechanisms, biosensors, and biofuels.

References

1. *Annual Energy Review*, U.S.E.I. Administration, Editor 2011.
2. Stephanopoulos, G., *Challenges in engineering microbes for biofuels production.* Science, 2007. **315**(5813): p. 801-4.
3. Goldemberg, J., et al., *Ethanol learning curve - the Brazilian experience.* Biomass & Bioenergy, 2004. **26**(3): p. 301-304.
4. Fischer, C.R., D. Klein-Marcuschamer, and G. Stephanopoulos, *Selection and optimization of microbial hosts for biofuels production.* Metab Eng, 2008. **10**(6): p. 295-304.
5. Lee, S.K., et al., *Metabolic engineering of microorganisms for biofuels production: from bugs to synthetic biology to fuels.* Curr Opin Biotechnol, 2008. **19**(6): p. 556-63.
6. Shi, S., et al., *Prospects for microbial biodiesel production.* Biotechnol J, 2011. **6**(3): p. 277-85.
7. Fortman, J.L., et al., *Biofuel alternatives to ethanol: pumping the microbial well.* Trends Biotechnol, 2008. **26**(7): p. 375-81.
8. Sims, R.E., et al., *An overview of second generation biofuel technologies.* Bioresour Technol, 2010. **101**(6): p. 1570-80.
9. Alper, H. and G. Stephanopoulos, *Engineering for biofuels: exploiting innate microbial capacity or importing biosynthetic potential?* Nat Rev Microbiol, 2009. **7**(10): p. 715-23.
10. Dunlop, M.J., *Engineering microbes for tolerance to next-generation biofuels.* Biotechnol Biofuels, 2011. **4**: p. 32.
11. *Help: Ribosome Binding Site.* Registry of Standard Biological Parts [cited 2012 July 17]; Available from: http://partsregistry.org/Help:Ribosome_Binding_Site.
12. Peralta-Yahya, P.P. and J.D. Keasling, *Advanced biofuel production in microbes.* Biotechnol J, 2010. **5**(2): p. 147-62.
13. Nicolaou, S.A., S.M. Gaida, and E.T. Papoutsakis, *A comparative view of metabolite and substrate stress and tolerance in microbial bioprocessing: From biofuels and chemicals, to biocatalysis and bioremediation.* Metab Eng, 2010. **12**(4): p. 307-31.
14. Sikkema, J., J.A. de Bont, and B. Poolman, *Mechanisms of membrane toxicity of hydrocarbons.* Microbiol Rev, 1995. **59**(2): p. 201-22.
15. Ramos, J.L., et al., *Mechanisms of solvent tolerance in gram-negative bacteria.* Annu Rev Microbiol, 2002. **56**: p. 743-68.
16. Dunlop, M.J., et al., *Engineering microbial biofuel tolerance and export using efflux pumps.* Mol Syst Biol, 2011. **7**: p. 487.
17. Van Hamme, J.D., A. Singh, and O.P. Ward, *Recent advances in petroleum microbiology.* Microbiol Mol Biol Rev, 2003. **67**(4): p. 503-49.
18. Wagner, S., et al., *Consequences of membrane protein overexpression in Escherichia coli.* Mol Cell Proteomics, 2007. **6**(9): p. 1527-50.

19. Holtwick, R., F. Meinhardt, and H. Keweloh, *cis-trans isomerization of unsaturated fatty acids: cloning and sequencing of the cti gene from Pseudomonas putida P8.* Appl Environ Microbiol, 1997. **63**(11): p. 4292-7.

20. Junker, F. and J.L. Ramos, *Involvement of the cis/trans isomerase Cti in solvent resistance of Pseudomonas putida DOT-T1E.* J Bacteriol, 1999. **181**(18): p. 5693-700.

21. Kabelitz, N., P.M. Santos, and H.J. Heipieper, *Effect of aliphatic alcohols on growth and degree of saturation of membrane lipids in Acinetobacter calcoaceticus.* FEMS Microbiol Lett, 2003. **220**(2): p. 223-7.

22. Topp, S. and J.P. Gallivan, *Riboswitches in unexpected places--a synthetic riboswitch in a protein coding region.* RNA, 2008. **14**(12): p. 2498-503.

23. Binder, S., et al., *A high-throughput approach to identify genomic variants of bacterial metabolite producers at the single-cell level.* Genome Biol, 2012. **13**(5): p. R40.

24. Kobayashi, H., et al., *Programmable cells: interfacing natural and engineered gene networks.* Proc Natl Acad Sci U S A, 2004. **101**(22): p. 8414-9.

25. Anesiadis, N., W.R. Cluett, and R. Mahadevan, *Dynamic metabolic engineering for increasing bioprocess productivity.* Metab Eng, 2008. **10**(5): p. 255-66.

26. Goldberg, S.D., et al., *Engineered single- and multi-cell chemotaxis pathways in E. coli.* Mol Syst Biol, 2009. **5**: p. 283.

27. Farmer, W.R. and J.C. Liao, *Improving lycopene production in Escherichia coli by engineering metabolic control.* Nat Biotechnol, 2000. **18**(5): p. 533-7.

28. Zhang, F., J.M. Carothers, and J.D. Keasling, *Design of a dynamic sensor-regulator system for production of chemicals and fuels derived from fatty acids.* Nat Biotechnol, 2012. **30**(4): p. 354-9.

29. Alon, U., *Network motifs: theory and experimental approaches.* Nat Rev Genet, 2007. **8**(6): p. 450-61.

30. Smits, W.K., O.P. Kuipers, and J.W. Veening, *Phenotypic variation in bacteria: the role of feedback regulation.* Nat Rev Microbiol, 2006. **4**(4): p. 259-71.

31. Grkovic, S., M.H. Brown, and R.A. Skurray, *Regulation of bacterial drug export systems.* Microbiol Mol Biol Rev, 2002. **66**(4): p. 671-701, table of contents.

32. van der Meer, J.R. and S. Belkin, *Where microbiology meets microengineering: design and applications of reporter bacteria.* Nat Rev Microbiol, 2010. **8**(7): p. 511-22.

33. Sorensen, S.J., M. Burmolle, and L.H. Hansen, *Making bio-sense of toxicity: new developments in whole-cell biosensors.* Curr Opin Biotechnol, 2006. **17**(1): p. 11-6.

34. Kaern, M., et al., *Stochasticity in gene expression: from theories to phenotypes.* Nat Rev Genet, 2005. **6**(6): p. 451-64.

35. Raser, J.M. and E.K. O'Shea, *Noise in gene expression: origins, consequences, and control.* Science, 2005. **309**(5743): p. 2010-3.

36. Dunlop, M.J., J.D. Keasling, and A. Mukhopadhyay, *A model for improving microbial biofuel production using a synthetic feedback loop.* Syst Synth Biol, 2010. **4**(2): p. 95-104.

37.   Lutz, R. and H. Bujard, *Independent and tight regulation of transcriptional units in Escherichia coli via the LacR/O, the TetR/O and AraC/I1-I2 regulatory elements.* Nucleic Acids Res, 1997. **25**(6): p. 1203-10.

38.   Poole, K., et al., *Expression of the multidrug resistance operon mexA-mexB-oprM in Pseudomonas aeruginosa: mexR encodes a regulator of operon expression.* Antimicrob Agents Chemother, 1996. **40**(9): p. 2021-8.

39.   Narita, S., et al., *Linkage of the efflux-pump expression level with substrate extrusion rate in the MexAB-OprM efflux pump of Pseudomonas aeruginosa.* Biochem Biophys Res Commun, 2003. **308**(4): p. 922-6.

40.   Alper, H., et al., *Tuning genetic control through promoter engineering.* Proc Natl Acad Sci U S A, 2005. **102**(36): p. 12678-83.

41.   Isken, S., et al., *Effect of organic solvents on the yield of solvent-tolerant Pseudomonas putida S12.* Appl Environ Microbiol, 1999. **65**(6): p. 2631-5.

42.   Li, X.Z., L. Zhang, and K. Poole, *Role of the multidrug efflux systems of Pseudomonas aeruginosa in organic solvent tolerance.* J Bacteriol, 1998. **180**(11): p. 2987-91.

43.   Evans, K., L. Adewoye, and K. Poole, *MexR repressor of the mexAB-oprM multidrug efflux operon of Pseudomonas aeruginosa: identification of MexR binding sites in the mexA-mexR intergenic region.* J Bacteriol, 2001. **183**(3): p. 807-12.

44.   Rutherford, B.J., et al., *Functional genomic study of exogenous n-butanol stress in Escherichia coli.* Appl Environ Microbiol, 2010. **76**(6): p. 1935-45.

45.   Paulsen, I.T., M.H. Brown, and R.A. Skurray, *Proton-dependent multidrug efflux systems.* Microbiol Rev, 1996. **60**(4): p. 575-608.

46.   Chen, H., et al., *The Pseudomonas aeruginosa multidrug efflux regulator MexR uses an oxidation-sensing mechanism.* Proc Natl Acad Sci U S A, 2008. **105**(36): p. 13586-91.

47.   Stiner, L. and L.J. Halverson, *Development and characterization of a green fluorescent protein-based bacterial biosensor for bioavailable toluene and related compounds.* Appl Environ Microbiol, 2002. **68**(4): p. 1962-71.

48.   Rojas, A., et al., *In vivo and in vitro evidence that TtgV is the specific regulator of the TtgGHI multidrug and solvent efflux pump of Pseudomonas putida.* J Bacteriol, 2003. **185**(16): p. 4755-63.

49.   Teran, W., et al., *Complexity in efflux pump control: cross-regulation by the paralogues TtgV and TtgT.* Mol Microbiol, 2007. **66**(6): p. 1416-28.

50.   Teran, W., et al., *Antibiotic-dependent induction of Pseudomonas putida DOT-T1E TtgABC efflux pump is mediated by the drug binding repressor TtgR.* Antimicrob Agents Chemother, 2003. **47**(10): p. 3067-72.

51.   Duque, E., et al., *Global and cognate regulators control the expression of the organic solvent efflux pumps TtgABC and TtgDEF of Pseudomonas putida.* Mol Microbiol, 2001. **39**(4): p. 1100-6.

52.   Kurth, E.G., et al., *Involvement of BmoR and BmoG in n-alkane metabolism in 'Pseudomonas butanovora'.* Microbiology, 2008. **154**(Pt 1): p. 139-47.

53.   Paitan, Y., et al., *Monitoring aromatic hydrocarbons by whole cell electrochemical biosensors.* Anal Biochem, 2004. **335**(2): p. 175-83.

54. Willardson, B.M., et al., *Development and testing of a bacterial biosensor for toluene-based environmental contaminants.* Appl Environ Microbiol, 1998. **64**(3): p. 1006-12.

55. Koutinas, M., et al., *The regulatory logic of m-xylene biodegradation by Pseudomonas putida mt-2 exposed by dynamic modelling of the principal node Ps/Pr of the TOL plasmid.* Environ Microbiol, 2010. **12**(6): p. 1705-18.

56. Phoenix, P., et al., *Characterization of a new solvent-responsive gene locus in Pseudomonas putida F1 and its functionalization as a versatile biosensor.* Environ Microbiol, 2003. **5**(12): p. 1309-27.

57. Jude, F., et al., *TbtABM, a multidrug efflux pump associated with tributyltin resistance in Pseudomonas stutzeri.* FEMS Microbiol Lett, 2004. **232**(1): p. 7-14.

58. Sun, X. and J.J. Dennis, *A novel insertion sequence derepresses efflux pump expression and preadapts Pseudomonas putida S12 for extreme solvent stress.* J Bacteriol, 2009. **191**(21): p. 6773-7.

59. Sun, X., et al., *An antirepressor, SrpR, is involved in transcriptional regulation of the SrpABC solvent tolerance efflux pump of Pseudomonas putida S12.* J Bacteriol, 2011. **193**(11): p. 2717-25.

60. Volkers, R.J.M., et al., *Isolation and genetic characterization of an improved benzene-tolerant mutant of Pseudomonas putida S12.* Environmental Microbiology Reports, 2010. **2**(3): p. 456-460.

61. Ratajczak, A., W. Geissdorfer, and W. Hillen, *Expression of alkane hydroxylase from Acinetobacter sp. Strain ADP1 is induced by a broad range of n-alkanes and requires the transcriptional activator AlkR.* J Bacteriol, 1998. **180**(22): p. 5822-7.

62. Canosa, I., et al., *A positive feedback mechanism controls expression of AlkS, the transcriptional regulator of the Pseudomonas oleovorans alkane degradation pathway.* Mol Microbiol, 2000. **35**(4): p. 791-9.

63. Sticher, P., et al., *Development and characterization of a whole-cell bioluminescent sensor for bioavailable middle-chain alkanes in contaminated groundwater samples.* Appl Environ Microbiol, 1997. **63**(10): p. 4053-60.

64. van Beilen, J.B., et al., *Analysis of Pseudomonas putida alkane-degradation gene clusters and flanking insertion sequences: evolution and regulation of the alk genes.* Microbiology, 2001. **147**(Pt 6): p. 1621-30.

65. Leahy, J.G., G.R. Johnson, and R.H. Olsen, *Cross-regulation of toluene monooxygenases by the transcriptional activators TbmR and TbuT.* Appl Environ Microbiol, 1997. **63**(9): p. 3736-9.

66. Selifonova, O.V. and R.W. Eaton, *Use of an ipb-lux Fusion To Study Regulation of the Isopropylbenzene Catabolism Operon of Pseudomonas putida RE204 and To Detect Hydrophobic Pollutants in the Environment.* Appl Environ Microbiol, 1996. **62**(3): p. 778-83.

67. Shetty, R.P., D. Endy, and T.F. Knight, Jr., *Engineering BioBrick vectors from BioBrick parts.* J Biol Eng, 2008. **2**: p. 5.

68. Gibson, D.G., et al., *Enzymatic assembly of DNA molecules up to several hundred kilobases.* Nat Methods, 2009. **6**(5): p. 343-5.

69. Kohanski, M.A., et al., *A common mechanism of cellular death induced by bactericidal antibiotics.* Cell, 2007. **130**(5): p. 797-810.

70. Sanli, G., S.I. Blaber, and M. Blaber, *Reduction of wobble-position GC bases in Corynebacteria genes and enhancement of PCR and heterologous expression.* J Mol Microbiol Biotechnol, 2001. **3**(1): p. 123-6.

71. Gustafsson, C., S. Govindarajan, and J. Minshull, *Codon bias and heterologous protein expression.* Trends Biotechnol, 2004. **22**(7): p. 346-53.

72. Plotkin, J.B. and G. Kudla, *Synonymous but not the same: the causes and consequences of codon bias.* Nat Rev Genet, 2011. **12**(1): p. 32-42.

73. Pini, C., et al., *Regulation of the cyclopropane synthase cfaB gene in Pseudomonas putida KT2440.* FEMS Microbiol Lett, 2011. **321**(2): p. 107-14.

Appendices

A.   Plasmid Maps
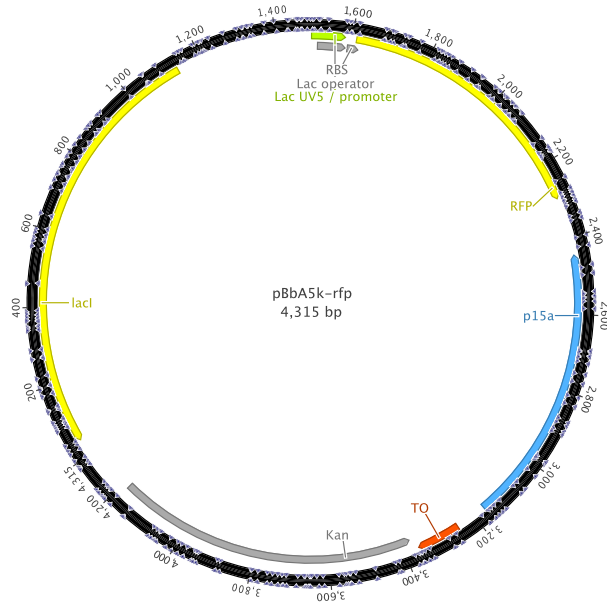
Figure A.1. Plasmid map of pBbA5k-rfp.
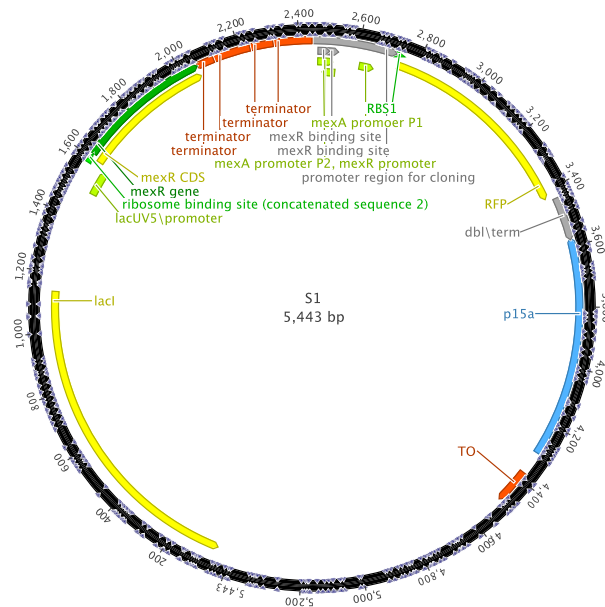
Figure A.2. Plasmid map of biosensor S1.
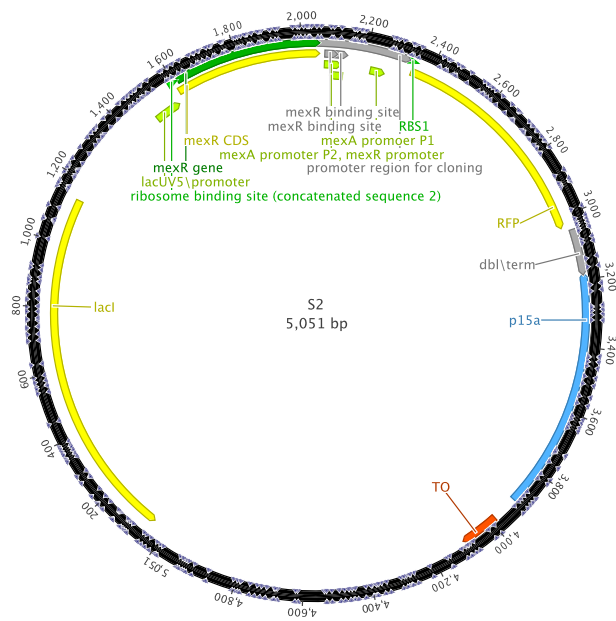
Figure A.3. Plasmid map of biosensor S2.
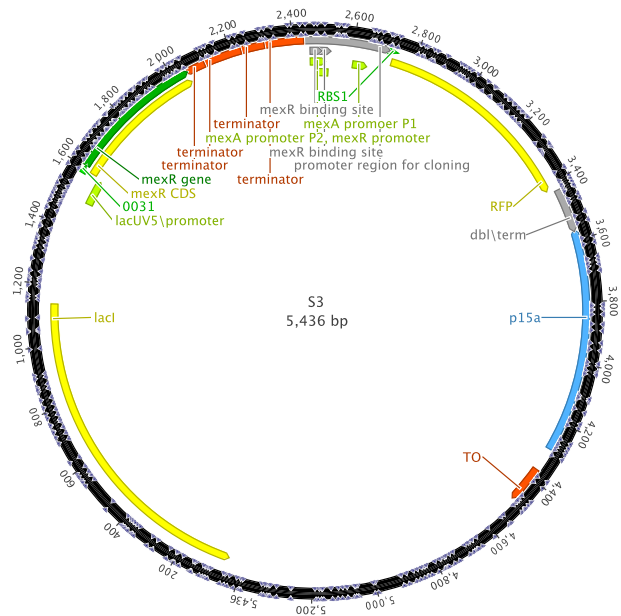
Figure A.4. Plasmid map of biosensor S3.
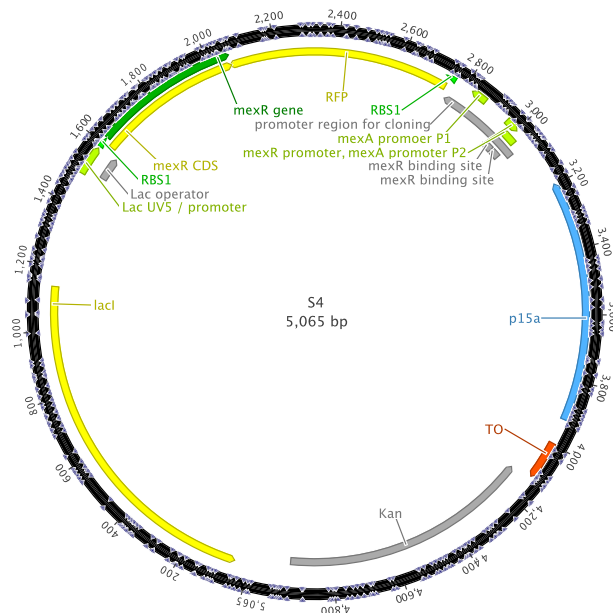
Figure A.5. Plasmid map of biosensor S4.
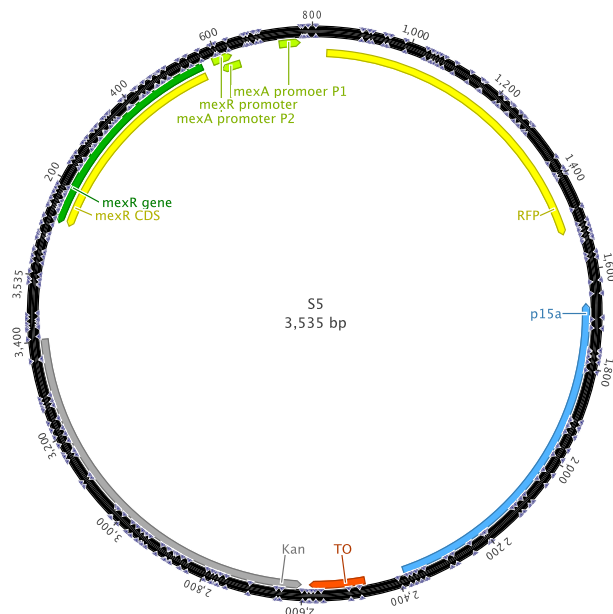
Figure A.6. Plasmid map of biosensor S5.
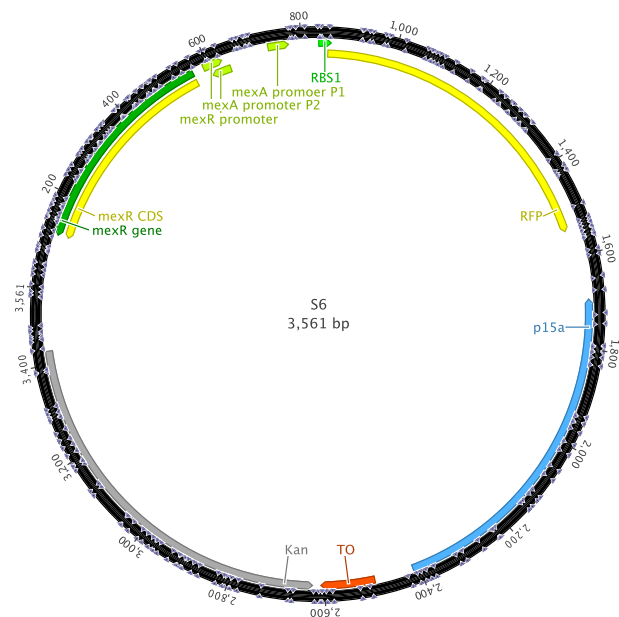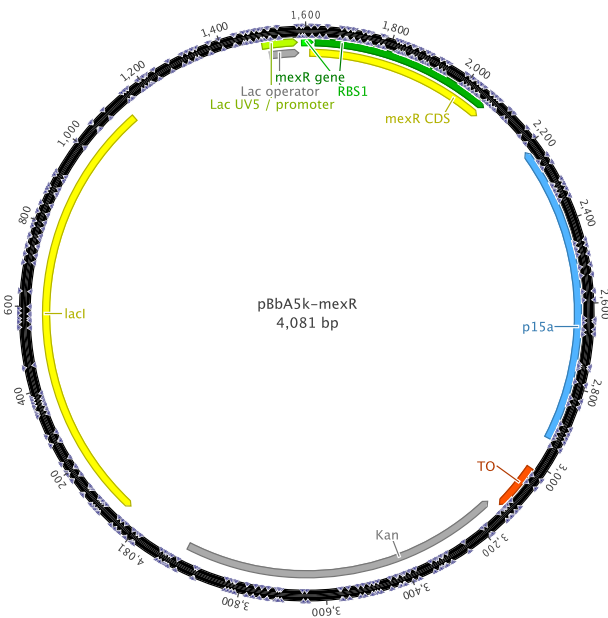
Figure A.7. Plasmid map of biosensor S6.

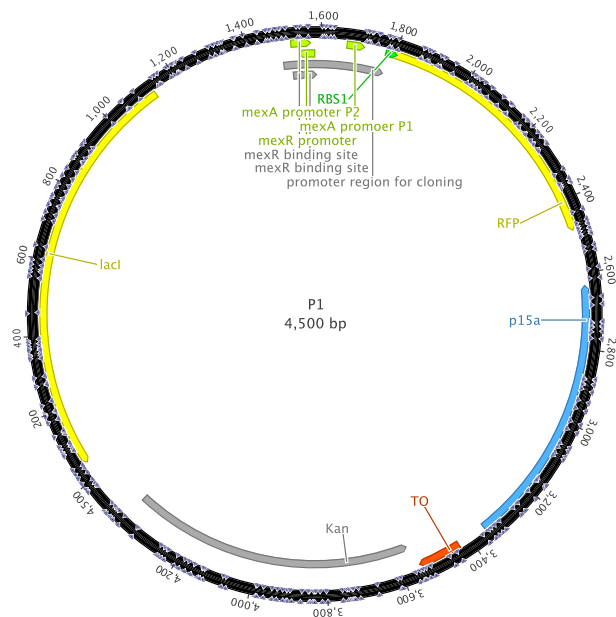Figure A.8. Plasmid map of negative control pBbA5k-mexR (N).

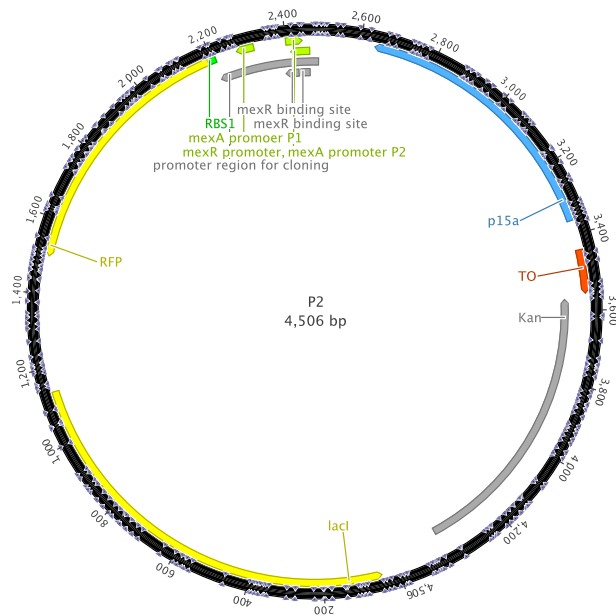Figure A.9. Plasmid map of positive control P1.
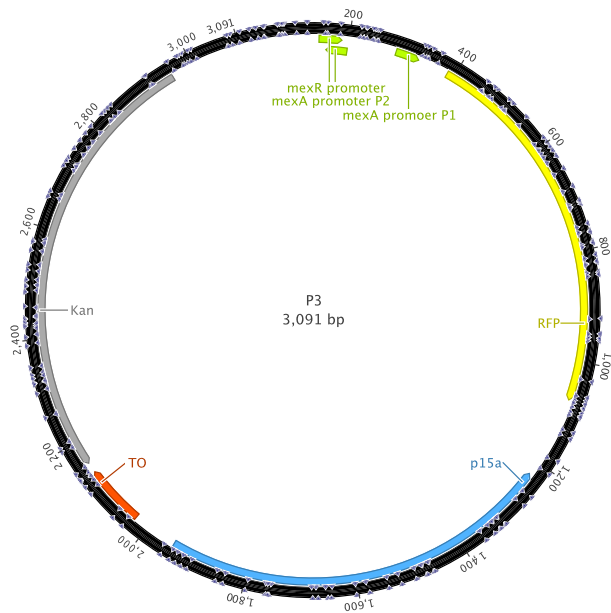

Figure A.10. Plasmid map of positive control P2.
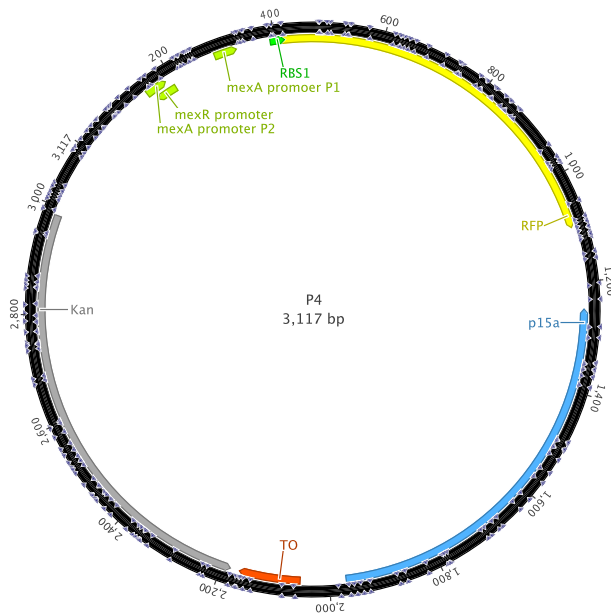
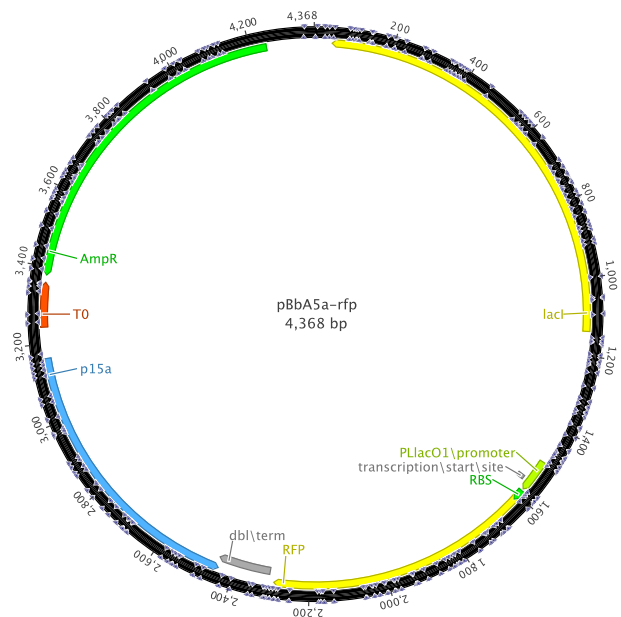Figure A.11. Plasmid map of positive control P3.

Figure A.12. Plasmid map of positive control P4.

Figure A.13. Plasmid map of pBbA5a-rfp.